Microscopic analysis of the superconducting quantum critical point: Finite-temperature crossovers in transport near a pair-breaking quantum phase transition

Nayana Shah
Department of Physics, University of Illinois at Urbana-Champaign, 1110 W. Green Street, Urbana, Illinois 61801, USA

Andrei Lopatin
Materials Science Division, Argonne National Laboratory, Argonne, Illinois 60439, USA
(Received 14 May 2007; published 14 September 2007)

A microscopic analysis of the superconducting quantum critical point realized via a pair-breaking quantum phase transition is presented. Finite-temperature crossovers are derived for the electrical conductivity, which is a key probe of superconducting fluctuations. By using the diagrammatic formalism for disordered systems, we are able to incorporate the interplay between fluctuating Cooper pairs and electrons, that is outside the scope of a time-dependent Ginzburg-Landau or effective bosonic action formalism. It is essential to go beyond the standard approximation in order to capture the zero-temperature correction which results purely from the (dynamic) quantum fluctuations and dictates the behavior of the conductivity in an entire low-temperature quantum regime. All dynamic contributions are of the same order and conspire to add up to a negative total, thereby inhibiting the conductivity as a result of superconducting fluctuations. On the contrary, the classical and the intermediate regimes are dominated by the positive bosonic channel. Our theory is applicable in one, two, and three dimensions and is relevant for experiments on superconducting nanowires, doubly connected cylinders, thin films, and bulk in the presence of magnetic impurities, magnetic field, or other pair breakers. A window of nonmonotonic behavior is predicted to exist as either the temperature or the pair-breaking parameter is swept.

DOI: 10.1103/PhysRevB.76.094511 PACS number(s): 74.40.+k, 74.78.−w, 74.78.Na, 72.15.−v

I. INTRODUCTION

The study of quantum phase transitions[1,2] has consistently been one of the frontier fields in condensed matter physics for the last decades. The steady growth in the possibility of simultaneously accessing lower temperatures and higher values of tuning parameters such as pressure and magnetic field, together with the possibility of operating old and new experimental techniques under such extreme conditions, has provided the necessary thrust. Discovery of new materials and physical systems has been another key factor. Not only has it maintained the freshness and novelty of the field but it has also helped to identify the universal features. Complex materials usually go hand in hand with complex phase diagrams with many competing or coexisting orders, given the multitude of energy scales that they have. Although this accounts for a rich body of physics, it also makes it harder to unmask the universal features and to systematically explore the neighborhood of the quantum phase transitions in the system.

Technological advances in relatively recent years have made it possible to make precisely designed and controllable bulk, mesoscopic, and nanoscale systems, consisting of cold atoms and quantum dots, for example. These have not only opened other avenues for studying quantum phase transitions but also served as model systems where theoretical predictions can be verified with the help of tunable parameters. This, in turn, can act as a starting point for understanding complex materials which are not as easy to control.

By now, there is a large body of theoretical work devoted to studying quantum phase transitions in a whole range of systems ranging from heavy fermion compounds, high-temperature superconductors, manganites, and organic materials to quantum dot and cold atomic systems. Transitions between and out of different correlated states of matter ranging from magnetic, superconducting, and charge-ordered states to more exotic, fractional, and topological states have been the subject of research. In spite of active interest, many questions still remain unanswered.

To date, superconductivity remains one of the most striking examples of emergent many-body states and quantum phase transitions involving a superconducting state are ubiquitous in a whole variety of materials. In many cases, it appears as one of the multiple phases in a complex phase diagram, with its mechanism not always clearly understood. However, there is another set of materials consisting of single elements or simple compounds with relatively simple phase diagrams which too display superconductivity.

The BCS theory that was put forward exactly 50 years ago was able to explain the basic mechanism of superconductivity which, in turn, was discovered for the first time almost another 50 years earlier. This theory is one of the crowning glories of condensed matter physics and a prototype of an ideal many-body theory, which is successful in explaining the experimentally observed thermodynamic and electrodynamic behavior in a large class of materials which is commonly labeled as conventional or BCS superconductors.[3,4]

The point of view we want to take in this paper is to study the physics of quantum phase transitions in such a BCS superconductor for which the theory is well understood and experimental properties well characterized. The theory could then be cleanly tested by taking a conventional superconductor with a simple phase diagram. Such a study would exemplify the physics of a superconducting quantum phase

transition which is not only of fundamental and technological interest but also a prototype for quantum phase transitions in other correlated systems.

The key characteristic of the BCS theory is the pairing of electrons with their time-reversed partners to form a condensate of Cooper pairs that superconducts. As the temperature is increased, more and more quasiparticles are formed by exciting electrons out of the condensate by breaking the pairs, until superconductivity is destroyed at a mean-field transition temperature. The experimental transition temperature is well defined and the transition is mean-field-like in most conventional bulk superconductors. Superconducting fluctuations, however, do exist even beyond the transition temperature and the fluctuations become stronger as the dimensionality of the sample is reduced. The effect of fluctuating Cooper pairs on different physical properties such as diamagnetism, specific heat, and conductivity was actively studied—both theoretically and experimentally—about a decade after the BCS theory was put forward; see the review on fluctuation effects in Ref. 5 which was already written three decades ago. The interest in studying fluctuation effects saw a revival after the discovery of high-temperature superconductivity and corresponding theoretical results can be found in a more recent review article.[6]

What is the way to start from a superconducting state at the absolute zero of the temperature and destroy it at a finite value of some tuning parameter via a second order phase transition? One has to think of a way of breaking the pairs without the help of thermal fluctuations. It turns out that all one has to do is to turn on a perturbation that breaks the time-reversal symmetry. Pair-breaking perturbations resulting in a suppression of the transition temperature have been well understood and it has been known for a long time that superconductivity is destroyed even at zero temperature once the pair-breaking parameter reaches a critical strength. We recognize such pair-breaking quantum phase transitions (with dynamic critical exponent $z=2$) out of a superconducting state as an important class of quantum phase transitions and make it the subject of our study.

In spite of the long history of superconducting fluctuation effects near the classical transition, there has been no systematic theoretical analysis of such effects in the vicinity of a pair-breaking quantum phase transition. In this paper, we have used the finite-temperature Matsubara diagrammatic method to evaluate the fluctuation corrections to the electrical conductivity which is one of the key physical quantities capable of diagnosing and showcasing the role of superconducting fluctuations. We have incorporated the (dynamic) quantum fluctuations by going beyond the standard approximations and mapped out the fluctuation regimes near the transition. Such a study is timely given the progress in fabricating ultranarrow superconducting nanowires and doubly connected cylinders in addition to thin-film samples. Not only will it allow identifying the universal features near superconducting quantum phase transitions in complex materials but it will also play a crucial role in enhancing our understanding of mesoscopic superconductivity. The microscopic approach we use allows us to treat the fluctuation corrections involving the interaction between the electrons and the fluctuating Cooper pairs and identify the regimes in which they dominate. Our analysis can then serve as a guideline for the construction and validation of an effective bosonic theory or a time-dependent Ginzburg-Landau formalism which does not incorporate the electrons. Such a bosonic theory can then be used for further analysis of the quantum critical point especially in one and two dimensions, given that the upper critical dimension in our case is 2.

The outline of the paper is as follows: In Sec. II, we lay the foundation for the remainder of the paper by clearly defining the meaning of a pair-breaking perturbation and introducing the class of pair-breaking quantum phase transitions that are of interest to us. We present the framework based on Usadel equations as a systematic and general method for obtaining the expression for the pair-breaking parameter in a given situation and illustrate it by considering some examples which are simple yet relevant to our analysis.

In Sec. III, we present the calculation of the fluctuation corrections to the normal state conductivity in the vicinity of the pair-breaking phase transition. We introduce the key building blocks of the temperature diagrammatic perturbation theory that we need, show how they are modified in the presence of a pair-breaking perturbation, and present their limiting forms. A fairly detailed account of the actual evaluation of diagrams corresponding to the fluctuation corrections is then given, focusing on the careful considerations required in order to incorporate the quantum (dynamic) fluctuations correctly. The results of this section are applicable near the entire phase transition line, starting from the classical finite-temperature transition in the absence of pair-breaking perturbation to the quantum phase transition driven by tuning the pair-breaking parameter at zero temperature.

The evaluation of these general expressions in the vicinity of the quantum phase transition is done in Sec. IV. Once the dominant corrections are identified, we present the different fluctuation regimes that come out of our analysis. There are three regimes—quantum, intermediate, and classical—and the behavior of the conductivity depends on the path of approach to the quantum phase transition. We demonstrate how these results vary based on the effective dimensionality of the problem and provide predictions of our theory that should be applicable to experiments on nanowires or doubly connected cylinders, thin films, and bulk systems. The result we obtain by evaluating the "Aslamazov-Larkin" correction in the vicinity of the classical transition is given as a benchmark to compare with the well-established results in the literature and also with its behavior near the quantum phase transition.

In the final section, we place our work in a bigger picture by discussing related theoretical and experimental work. Different theoretical approaches for the same problem as well as slightly different physical configurations studied using a formalism similar to ours are both included. An attempt to interpret all the experiments on superconducting quantum phase transition in thin films would clearly be outside the scope of this paper. We have hence focused mainly on those that have analyzed the data in terms of quantum corrections, including the fluctuation corrections. Relevant experiments on superconducting nanowires and doubly connected cylinders are relatively scant so far. However, we discuss the current status to support our belief that given the technological

advances in the recent years, the predictions of our theory should not only be accessible but also important from the point of view of using ultranarrow wires in superconducting electronic circuits.

II. PAIR-BREAKING PARAMETER (α)

A. Definition and physical meaning

A pair-breaking perturbation is any perturbation that breaks the time-reversal degeneracy of a superconducting paired state. Anderson's theorem[7] asserts that in the absence of such a perturbation, the superconducting critical temperature T_c and the BCS density of states remain the same even after alloying the superconductor with impurities. However, if the impurities are magnetic, Abrikosov and Gor'kov[8] found that the T_c is suppressed and the density of states is modified as well (giving a gapless regime). They parametrized the strength of the pair-breaking perturbation by a *pair-breaking parameter* α and obtained

$$\ln\left(\frac{T_c}{T_{c0}}\right) = \psi\left(\frac{1}{2}\right) - \psi\left(\frac{1}{2} + \frac{\alpha}{2\pi T_c}\right), \tag{1}$$

where ψ is the digamma function and $T_{c0} \equiv T_c(\alpha=0)$. The parameter α was shown to be inverse of the spin-flip scattering time which is proportional to the density of magnetic impurities.

Following this classic work, it was recognized that the above equation for T_c suppression (as well as gapless superconductivity) can be transcribed for a whole class of pair-breaking perturbations for which the transition to the normal state in the presence of α is of second order, once the appropriate α is used for each case.[3,4] What is essential is the presence of a rapid scattering mechanism that modulates over time the pair-breaking perturbation seen by a given Cooper pair of electrons, assuring an *ergodic* behavior of electrons. Then, α can be interpreted as the depairing energy (energy splitting) of a pair of time-reversed electrons, averaged over a time interval τ_K it takes for their relative phase to be randomized by the perturbation; one thus has $2\alpha \equiv \hbar/\tau_K$.

This generalization of the concept of pair-breaking offers the possibility of defining a pair-breaking parameter not only for bulk systems but also for mesoscopic and nonhomogeneous systems and for situations in which multiple pair-breaking mechanisms might be operative. However, the derivation of α might not be straightforward in such cases. Below, we will describe the Usadel equation formalism as a general method to derive α for a given configuration.

B. Derivation using Usadel equations

In this paper, we are interested in focusing on dirty superconductors for which the Usadel equation formalism[9,10] is well suited. Writing the Heisenberg equation of motion starting from the BCS Hamiltonian, one gets the microscopic Gorkov equations for the normal and anomalous Green functions. Using the fact that the characteristic length scale for the normal state is smaller than the length scale for the superconducting order parameter variation, one can make the quasiclassical approximation

$$\frac{\hbar/p_F}{\xi_0} \sim \frac{\Delta}{E_F} \ll 1 \tag{2}$$

(which is quite accurate for most classic low-temperature superconductors and less so for high-temperature superconductors) to exclude the fast oscillations of the Green functions associated with variations of the relative coordinate on a scale $\hbar/p_F$ and rewrite the Gorkov equations in terms of the quasiclassical Green functions with only a slow dependence on the center-of-mass coordinate varying on the scale ξ_0. The Eilenberger equations so derived can be further simplified in the dirty limit

$$\frac{l}{\xi_0} \sim \frac{\tau}{\hbar/T_c} \ll 1 \tag{3}$$

(where l is the mean free path and τ is the mean free impurity scattering time), in which the strong scattering by impurities produces averaging over momentum directions, to obtain the Usadel equations[9]

$$-iD\left[g\left(\nabla - \frac{2ie}{c}\mathbf{A}\right)^2 f - f\nabla^2 g\right] = 2\Delta g - 2i\omega_n f, \tag{4}$$

$$-iD\left[g\left(\nabla + \frac{2ie}{c}\mathbf{A}\right)^2 f^\dagger - f^\dagger\nabla^2 g\right] = 2\Delta^* g - 2i\omega_n f^\dagger, \tag{5}$$

where $D = v_F^2\tau/3$ is the three-dimensional diffusion constant. Note that g and f, the quasiclassical Green functions averaged over momentum directions, get expressed as functionals of the fluctuating order parameter field $\Delta(x,\tau)$. Below, we outline the precise recipe for deriving the pair-breaking parameter, starting from these equations.

To identify the pair-breaking parameter, it is enough to consider the Usadel equations for the f function to the lowest order in Δ, so as to obtain

$$-iDg_0\left(\nabla - \frac{2ie}{c}\mathbf{A}\right)^2 f = -2i\omega f + 2\Delta g_0, \tag{6}$$

with $g_0 = \text{sign}\ \omega$. One could interpret the depairing parameter as the lowest eigenvalue of the operator (in the transverse direction)

$$-\frac{D}{2}\left(\nabla_\perp - \frac{2ie}{c}\mathbf{A}\right)^2 f = \alpha f \tag{7}$$

obtained by appropriately choosing the gauge and the boundary conditions (to ensure absence of current perpendicular to a wire or film surface, for example). Alternatively, one can solve Eq. (6) for f and read out the expression for α from it. In the remaining part of this subsection, we illustrate the procedure for some examples of interest. The formalism is general enough and can be appropriately adapted to complicated situations involving the simultaneous occurrence of multiple pair-breaking perturbations.

Although the pair-breaking parameter for the classic example of magnetic impurities can be derived within the Eilenberger-Usadel formalism, we refer the reader to the original paper[8] and proceed to discuss some other specific examples.

1. Thin film

Consider a thin film with thickness s smaller than the superconducting coherence length ξ such that the superconducting fluctuations are effectively two dimensional ($d=2$). Let us focus on the orbital pair-breaking effect of a magnetic field H applied parallel to the film. We consider s to be smaller than the penetration depth λ so that one can assume the field to be uniform inside the sample. If the film is placed in the xy plane and H is parallel to the y axis, we choose the gauge such that $A_x=Hz$, $A_y=A_z=0$, where z is measured from the midplane of the film. Now, Eq. (6) takes the form

$$-i\frac{D}{2}\left[\frac{\partial^2}{\partial z^2}+\left(\frac{2ie}{c}Hz\right)^2\right]f=-i|\omega|f+\Delta, \tag{8}$$

which on integrating over the transverse direction (i.e., over z) leads to

$$iD\left(\frac{eH}{c}\right)^2\frac{s^3}{6}f=-i|\omega|fs+s\Delta \tag{9}$$

on using the appropriate boundary conditions that require the transverse derivative of f to vanish on the surface of the film. We thus have

$$f=\frac{-i\Delta}{|\omega|+\alpha}, \tag{10}$$

with

$$\alpha=\frac{D}{6}\left(\frac{eHs}{c}\right)^2, \tag{11}$$

identified as the pair-breaking parameter.

2. Nanowire

Consider a wire of radius R such that the diameter is smaller than ξ and λ and the effective dimensionality of the problem is $d=1$ as far as the superconducting fluctuations are concerned. To obtain the expression for the pair-breaking parameter coming from the orbital effect of a magnetic field H applied parallel to the wire, we use the cylindrical coordinates and choose the gauge such that $A_\phi=H\rho/2$, $A_\rho=A_z=0$. For the sake of illustration, this time we start with Eq. (7) which takes the form

$$\frac{D}{2}\left[-\frac{1}{\rho}\frac{\partial}{\partial\rho}\left(\rho\frac{\partial}{\partial\rho}\right)+\left(\frac{eH\rho}{c}\right)^2\right]f=\alpha f, \tag{12}$$

and on integrating in the transverse direction (i.e., over ρ) gives

$$\frac{D}{2}f\int_0^R\rho d\rho\left(\frac{eH\rho}{c}\right)^2=\alpha f\int_0^R\rho d\rho \tag{13}$$

using the boundary conditions that require $\partial f/\partial\rho$ to vanish at $\rho=R$. The expression for the pair-breaking parameter,

$$\alpha=\frac{D}{4}\left(\frac{eHR}{c}\right)^2, \tag{14}$$

is then immediately evident.

If one considers a magnetic field applied perpendicular to the wire, the pair-breaking parameter is given by

$$\alpha=\frac{D}{2}\left(\frac{eHR}{c}\right)^2 \tag{15}$$

instead and the calculation follows on the lines similar to that for a field applied parallel to a film.

3. Doubly connected cylinder

Consider a doubly connected (hollow) cylinder with inner radius r_1 and outer radius r_2 such that the wall of the cylinder is thinner than ξ and λ and the effective dimensionality is $d=1$ as for the case of a nanowire. Due to the single-valuedness of Δ and f, their ϕ dependence is given by $e^{in\phi}$, where n is an arbitrary integer. Choosing the cylindrical gauge

$$\mathbf{A}=\frac{1}{2}\mathbf{h}\times\mathbf{r}=\frac{1}{2}\hat{\phi}h\rho, \tag{16}$$

as we did also for the nanowire, Eq. (7) becomes

$$\frac{D}{2}\left[-\frac{1}{\rho}\frac{d}{d\rho}\left(\rho\frac{d}{d\rho}\right)+\left(\frac{m}{\rho}-\frac{eh\rho}{c}\right)^2\right]f=\alpha f. \tag{17}$$

Integrating over the radial direction (from r_1 to r_2), we obtain the expression

$$\alpha=D\left\{\frac{eH}{4c}\left[-4n+\frac{eH}{c}(r_1^2+r_2^2)\right]+n^2\frac{\ln(r_2/r_1)}{r_2^2-r_1^2}\right\}, \tag{18}$$

where n is an arbitrary integer (note that for $r_1=0$, we correctly recover the result for the nanowire). For a thin cylinder ($r_1\approx r_2\approx r$), the pair-breaking parameter reduces to

$$\alpha=(D/2r^2)(\Phi/\Phi_0-n)^2, \tag{19}$$

where Φ is the flux enclosed by the cylinder, thereby rendering the classic Little-Park oscillations[3] of T_c as can be seen from Eq. (1). Interestingly, for a cylinder with small enough radius, $r<r_c=\sqrt{D\gamma/4\pi T_{c0}}$, it is possible to push the T_c down to zero at magnetic fields corresponding to half-integer fluxes $\Phi=\Phi_0(1/2+n)$.

C. Pair-breaking phase transition

By substituting Eq. (10) for f in the presence of α into the self-consistency equation for the order parameter, one can obtain the transition temperature in the same way as it is obtained in the absence of a pair-breaking parameter. The boundary between the superconducting and normal states in the α-T plane is given by

$$\ln\left(\frac{T}{T_{c0}}\right)=\psi\left(\frac{1}{2}\right)-\psi\left(\frac{1}{2}+\frac{\alpha}{2\pi T}\right), \tag{20}$$

as is shown in Fig. 1. At a given pair-breaking strength α, superconductivity is destroyed at $T=T_c(\alpha)$ and at a given temperature T, at $\alpha=\alpha_c(T)$, obtained by solving Eq. (20) for T and for α, respectively. In the absence of a pair-breaking perturbation ($\alpha=0$), the system undergoes the classical tran-

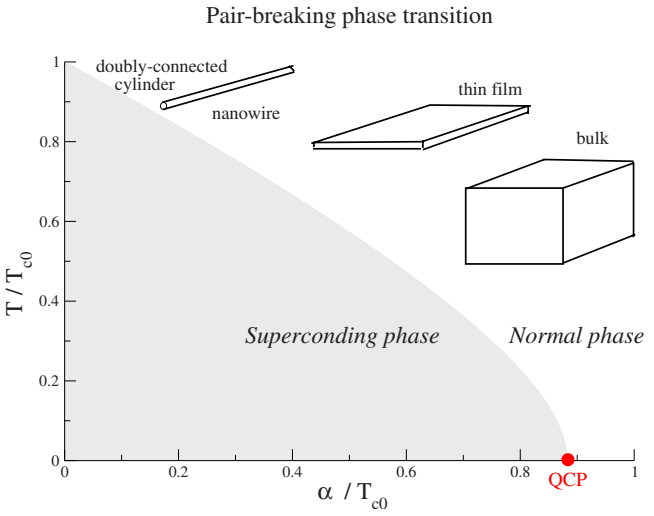

FIG. 1. (Color online) Phase diagram showing the pair-breaking transition from superconducting to normal state with the boundary given by Eq. (20). A superconducting quantum critical point (QCP) is seen to be realized when the pair-breaking parameter reaches a critical strength $\alpha_{c0}/T_{c0}=0.889$. Different systems of interest are also illustrated.

sition at $T_c(0)\equiv T_{c0}$. In the neighborhood of this classical transition, for $\alpha \ll T_{c0}$ we can define the quantity

$$\delta_T(\alpha,T) \equiv \frac{T - T_c(\alpha)}{T_c(\alpha)} \tag{21}$$

that measures the relative distance from the critical temperature $T_c(\alpha)$.

On the other hand, if the pair-breaking effect is sufficiently strong, superconductivity is destroyed even at $T=0$, thereby yielding a second order quantum phase transition. The critical value of α at zero temperature,

$$\alpha_{c0} \equiv \alpha_c(T=0) = \frac{\pi T_{c0}}{2\gamma},$$

can be obtained by using the first term in the asymptotic form of the digamma function for large arguments [$\psi(z) = \ln z$]. Here, $\ln \gamma \approx 0.577$ is the Euler constant and one can immediately see that $2\alpha_{c0}=1.76T_c=\Delta_0$, the BCS gap at zero temperature. Expanding the right hand side of Eq. (20) to next order in small T, one finds that the transition curve close to α_{c0} is given by

$$\alpha_c(T \ll \alpha_{c0}) = \alpha_{c0} - \frac{\pi^2 T^2}{6\alpha_{c0}}. \tag{22}$$

In the vicinity of the pair-breaking quantum phase transition, we will define the quantity

$$\delta_\alpha(\alpha,T) \equiv \frac{\alpha - \alpha_c(T)}{\alpha_c(T)}, \tag{23}$$

which can be interpreted as the relative distance from the critical pair-breaking strength $\alpha_c(T)$ at a given $T \ll \alpha_{c0}$.

In the following section, we will be interested in evaluating the fluctuation corrections to the normal state conductivity in the vicinity of a pair-breaking transition. The effective quasiclassical approach based on the Usadel equations that we have discussed in the previous subsection is quite accurate in the dirty limit and has no applicability restrictions in terms of the temperature range. To evaluate the fluctuation corrections, one could imagine using the functional formalism based on this approach. However, we have chosen to use the standard diagrammatic method instead.

III. SUPERCONDUCTING FLUCTUATION CORRECTIONS TO CONDUCTIVITY

We will carry out a microscopic calculation within the standard framework of temperature diagrammatic technique for a disordered electron system[11,12] in the diffusive limit ($\tau^{-1} \gg T, \alpha$). This technique has been extensively used in studying the weak localization[13] and electron-electron interaction[14] corrections to the conductivity in low-dimensional systems. In the same way as these corrections were studied also using alternative formalisms including the nonlinear sigma model,[15] it seems plausible to have an alternative derivation of the superconducting fluctuation corrections to the conductivity, which falls in the same league. Here, we will restrict ourselves solely to diagrammatic perturbation theory.

A. Basic ingredients

Although the framework we use is standard, we will briefly discuss all the ingredients we need mainly for two reasons. First, we want to precisely demonstrate the way in which the presence of a pair-breaking parameter modifies these ingredients (see Refs. 6 and 12). Second, we want to catalog all the expressions we need, including their limiting forms in the vicinity of the quantum phase transition.

1. Green's function

As is standard, we assume a random disorder potential $V(\mathbf{r})$ drawn from a Gaussian white noise (δ-correlated) distribution such that $\langle V(\mathbf{r})\rangle=0$ and $\langle V(\mathbf{r})V(\mathbf{r}')\rangle=\langle V^2\rangle\delta(\mathbf{r}-\mathbf{r}')$. In the diagrams, a dashed line denotes

$$\langle V^2\rangle = \frac{1}{2\pi\nu\tau}, \tag{24}$$

where ν is the density of states at the Fermi level and τ^{-1}, as defined earlier, is the frequency of elastic collisions. The single-electron Green function—denoted by a full line in the diagrams of Fig. 2—is given by

$$G(\omega_n,\mathbf{p}) = \frac{1}{i\left(\omega_n + \frac{\mathrm{sign}(\omega_n)}{2\tau}\right) - \xi_{\mathbf{p}}}, \tag{25}$$

where $\xi_{\mathbf{p}}$ is the single particle excitation spectrum measured from the chemical potential.

2. Cooperon

Diffuson and *Cooperon* are the key correlators, represented by a sum over ladder diagrams involving coherent scattering by impurities, in the particle-hole and particle-particle channel, respectively, the latter being of interest to us in the context of superconducting fluctuations. The expression for Cooperon—represented by a shaded rectangular block in the diagrams—in the presence of a pair-breaking parameter α is given by

$$C(\omega_n,\omega_m,\mathbf{q}) = \frac{2\pi\nu\theta(-\omega_n\omega_m)}{|\omega_n-\omega_m|+2\alpha_q}, \tag{26}$$

where $\theta(x)$ is the Heaviside theta function and

$$\alpha_q \equiv \alpha + Dq^2/2. \tag{27}$$

Here, ω_n is a fermionic Matsubara frequency and $\mathbf{q}$ is the momentum in the effective dimension as far as the superconducting fluctuations are concerned (note that D is the diffusion constant in three dimensions as long as the diffusion is still three dimensional).

Coherent scattering on the same impurity, by both the electrons forming a fluctuating Cooper pair, leads to renormalization of the vertex part in the particle-particle channel, given by

$$\lambda(\omega_n,\omega_m,\mathbf{q}) = \frac{C(\omega_n,\omega_m,\mathbf{q})}{2\pi\nu\tau}. \tag{28}$$

In the diagrams shown in Fig. 2, we denote λ by a shaded triangle.

3. Fluctuation propagator

The main building block of the diagrammatic technique that encodes the BCS superconducting interaction is the so-called *fluctuation propagator* (represented by a wavy line in the diagrams). It is the impurity-averaged sum over the ladder diagrams corresponding to the electron-electron interaction in the Cooper channel. The expression in the presence of α, obtained using Eq. (26) in a standard way, is given by

$$K^{-1}(|\Omega_\nu|,\mathbf{q}) = \ln\left(\frac{T}{T_{c0}}\right) - \psi\left(\frac{1}{2}\right) + \psi\left(\frac{1}{2}+\frac{\alpha_q+|\Omega_\nu|/2}{2\pi T}\right), \tag{29}$$

where Ω_ν is a bosonic Matsubara frequency.

The pole of Eq. (29) for q, $\Omega_\nu=0$ traces the boundary between the superconducting and normal phases (see Sec. II C). In the limit of zero pair-breaking strength ($\alpha=0$) and near the classical transition, $T\sim T_{c0}$, one can show that the expression for the fluctuation propagator reduces to

$$K^{-1}(|\Omega_\nu|,q) = \delta_T(0,T) + \frac{Dq^2+|\Omega_\nu|}{4\pi T}\psi'\left(\frac{1}{2}\right), \tag{30}$$

where $\psi'(1/2)=\pi^2/2$ and $\delta_T(\alpha,T)$ is defined earlier by Eq. (21).

On the other hand, at low temperatures, $T\ll\alpha_{c0}$, the fluctuation propagator can be reduced to the form

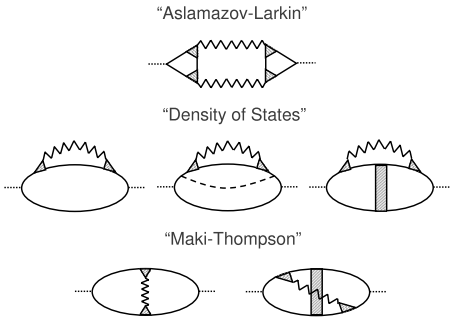

FIG. 2. Diagrams for the fluctuation conductivity divided into three groups. There is one diagram corresponding to the positive "Aslamazov-Larkin" correction. Three diagrams correspond to the negative "density-of-states" corrections, and each of them has two possible ways of putting arrows on the electron Green functions. There are two diagrams corresponding to the "Maki-Thompson" interference correction with no prescribed sign, the second of which has two ways of putting the arrows. Full lines stand for the disorder averaged normal state Green's function, wavy lines for the fluctuation propagator K, the shaded rectangles for the Cooperon C, and shaded triangles for the vertex $C/2\pi\nu\tau$.

$$K^{-1}(|\Omega_\nu|,\mathbf{q}) = \ln\left[\frac{\alpha_q+|\Omega_\nu|/2}{\alpha_c(T)}\right], \tag{31}$$

which correctly reproduces the transition curve $\alpha=\alpha_c(T)$. In certain regimes (see below), it is legitimate to expand the logarithm and get an even simpler expression,

$$K(|\Omega_\nu|,\mathbf{q}) = \frac{1}{\delta_\alpha(\alpha,T)+\dfrac{Dq^2+|\Omega_\nu|}{2\alpha_c(T)}}, \tag{32}$$

where $\delta_\alpha(\alpha,T)$ is given by Eq. (23).

B. Evaluation of the diagrams

The boundary between the superconducting and normal regions in the α-T phase diagram is given by Eq. (20) (see Fig. 1). Even while superconductivity is destroyed, superconducting fluctuations continue to persist in the normal state region and modify the normal state conductivity. We will evaluate the corrections to the conductivity coming from superconducting fluctuations using the standard Kubo formalism for linear response.[11] The electromagnetic response operator $Q(\Omega_\mu)$ is evaluated and the external frequency is analytically continued into the upper half-plane of the complex frequency ($i\Omega_\mu\to\Omega$). The fluctuation conductivity can then be obtained using

$$\delta\sigma(\Omega) = \lim_{\Omega\to 0}\frac{Q(-i\Omega)}{-i\Omega} \tag{33}$$

once the appropriate $Q(\Omega_\mu)$ has been evaluated.

In what follows, we will evaluate $Q(\Omega_\mu)$ using a standard set of diagrams.[6] As shown in Fig. 2, these diagrams can be divided into three groups based on their physical interpretation. Of these, the Aslamazov-Larkin (AL) type of correction[16] is the most intuitive. It is a positive contribution

coming from additional charge transfer via fluctuating Cooper pairs. The negative "density-of-states" (DOS) correction results from the reduction of the normal single-electron density of states at the Fermi level after accounting for the electrons participating in fluctuating Cooper pairs. The corresponding diagrams have only one electron line affected by the fluctuation propagator. The third, and the more indirect, correction is given by the "Maki-Thompson" (MT)[17–19] diagrams which could be thought to be originating from coherent Andreev scattering off the fluctuating pairs. One can see in Fig. 2 that the fluctuation propagator brings about interference between the electron lines.

Let us start by considering evaluation of the Aslamazov-Larkin diagram. The effective triangular vertex on either side (both yield the same final expression) is given by

$$\Gamma(\Omega_{1\nu},\Omega_\mu,\mathbf{q}) = eT\sum_{\omega_n,\mathbf{p}} \mathbf{p}_x \lambda(-\omega_n+\Omega_{1\nu},\omega_n-\Omega_\mu,\mathbf{q}) \times G(-\omega_n+\Omega_{1\nu},-\mathbf{p}+\mathbf{q})G(\omega_n-\Omega_\mu,\mathbf{p}) \times G(\omega_n,\mathbf{p})\lambda(\omega_n,-\omega_n+\Omega_{1\nu},\mathbf{q}) \quad (34)$$

(having chosen the x direction for concreteness). The presence of Heaviside θ functions in the expression for the vertex renormalizations λ, defined by Eqs. (26) and (28), dictates the possible signs and ranges of different frequencies. Taking these into account and by making simplifications valid in the small q and ω_n, $\Omega_{1\nu}$, $\Omega_\mu \ll \tau^{-1}$ limit of interest to us, we find a rather compact expression,

$$\Gamma(\Omega_{1\nu},\Omega_\mu,\mathbf{q}) = vD\mathbf{q}_x B(\Omega_{1\nu},\Omega_\mu), \quad (35)$$

with

$$B(\Omega_{1\nu},\Omega_\mu) = [\tilde{\psi}(|\Omega_{1\nu}|,\Omega_\mu) + \tilde{\psi}(|\Omega_\mu-\Omega_{1\nu}|,\Omega_\mu)] \quad (36)$$

and

$$\tilde{\psi}(w,z) \equiv \frac{1}{z}\left[\psi\left(\frac{1}{2}+\frac{\alpha_q+\frac{w+z}{2}}{2\pi T}\right)-\psi\left(\frac{1}{2}+\frac{\alpha_q+\frac{w}{2}}{2\pi T}\right)\right], \quad (37)$$

where $\psi(z)$ is the digamma function.

To evaluate the entire AL diagram, let us consider the summation over the internal bosonic frequency,

$$I(\Omega_\mu) \equiv T\sum_{\Omega_{1\nu}} B(\Omega_{1\nu},\Omega_\mu)^2 K(|\Omega_{1\nu}|)K(|\Omega_{1\nu}-\Omega_\mu|), \quad (38)$$

and write it as contour integration in a standard way (note that we have temporarily suppressed the $\mathbf{q}$ dependence in the fluctuation propagator K for the sake of compactness). By taking into account the analyticity of the integrand, the evaluation of I is reduced to an integration across two branch cuts (see Ref. 6). After combining terms and analytically continuing the external frequency to the upper half-plane ($i\Omega_\mu \to \Omega$), one finds that

$$I \equiv I_a + I_b, \quad (39)$$

with

$$I_a = -\frac{1}{4\pi i}\frac{\Omega}{2T}\int \frac{d\Omega_1}{\sinh^2\frac{\Omega_1}{2T}} K(-i\Omega_1)K(i\Omega_1) \times[\tilde{\psi}(-i\Omega_1,-i\Omega)+\tilde{\psi}(i\Omega_1,-i\Omega)]^2 \quad (40)$$

and

$$I_b = \frac{2}{4\pi i}\int d\Omega_1 \coth\frac{\Omega_1}{2T} K(-i\Omega_1-i\Omega)K(-i\Omega_1) \times[\tilde{\psi}(-i\Omega_1-i\Omega,-i\Omega)+\tilde{\psi}(-i\Omega_1,-i\Omega)]^2. \quad (41)$$

Since the contribution to the conductivity [Eq. (33)] goes as I/Ω, we need only consider the terms in I that are linear in Ω since we are interested in the $\Omega \to 0$ limit; terms that are zeroth order in Ω will be canceled by analogous terms in the remaining diagrams to ensure the absence of anomalous diamagnetism in the normal state. Carrying out an expansion in Ω, we can write

$$\tilde{\psi}(-i\Omega_1,-i\Omega) \to \frac{1}{4\pi T}\psi'\left(\frac{1}{2}+\frac{\alpha_q-i\Omega_1/2}{2\pi T}\right) - \frac{1}{2}\frac{i\Omega}{(4\pi T)^2}\psi''\left(\frac{1}{2}+\frac{\alpha_q-i\Omega_1/2}{2\pi T}\right). \quad (42)$$

Since I_a is already linear in Ω, in it we need only keep the zeroth order term from this expansion. On the other hand, using the expansion for both K and $\tilde{\psi}$, we have

$$I_b = \frac{-\Omega}{2\pi}\int d\Omega_1 \coth\frac{\Omega_1}{2T}\left[4\tilde{\psi}(-i\Omega_1)^2 K'(-i\Omega_1)K(-i\Omega_1) + \psi'\left(\frac{1}{2}+\frac{\alpha_q-\frac{i\Omega_1}{2}}{2\pi T}\right)\psi''\left(\frac{1}{2}+\frac{\alpha_q-\frac{i\Omega_1}{2}}{2\pi T}\right)\frac{K(-i\Omega_1)^2}{(2\pi T)^3}\right]. \quad (43)$$

We can integrate the first term by parts, combine similar terms from I_a and I_b, and after some manipulation get a final expression for I. One can then immediately write down the Aslamazov-Larkin fluctuation correction to conductivity as a sum of two terms:

$$\delta\sigma^{AL} = \delta\sigma^{AL}_{sh} + \delta\sigma^{AL}_{cth}, \quad (44)$$

where

$$\delta\sigma^{AL}_{sh} = \frac{D^2e^2}{2\pi Td}\int \frac{d^dq}{(2\pi)^d}\frac{d\Omega_1}{\sinh^2\frac{\Omega_1}{2T}} \times(\{\mathrm{Im}[K(-i\Omega_1,q)\gamma(-i\Omega_1,\mathbf{q})]\}^2 + \mathrm{Im}[K(-i\Omega_1,q)\gamma(-i\Omega_1,\mathbf{q})^2]\mathrm{Im}[K(-i\Omega_1,q)]) \quad (45)$$

and

$$\delta\sigma_{cth}^{AL} = \frac{D^2e^2i}{8\pi^4T^3}\int \frac{d^dqd\Omega_1}{(2\pi)^d}\coth\frac{\Omega_1}{2T}q_x^2K^2(-i\Omega_1,q) \times \psi'\left(\frac{1}{2}+\frac{\alpha_q-i\Omega_1/2}{2\pi T}\right)\psi'\left(\frac{1}{2}+\frac{\alpha_q-i\Omega_1/2}{2\pi T}\right), \tag{46}$$

with

$$\gamma(-i\Omega_1,\mathbf{q}) = \frac{\mathbf{q}}{2\pi T}\psi'\left(\frac{1}{2}+\frac{\alpha_q-i\Omega_1/2}{2\pi T}\right). \tag{47}$$

Going through the derivation, the reader can readily convince herself or himself that the contribution $\delta\sigma_{cth}^{AL}$ would be missed if one were to make the so-called static approximation in the effective vertex and use $\Gamma(\Omega_{1\nu}=0,\Omega_\mu,\mathbf{q})$ in the evaluation of the Aslamazov-Larkin diagram. As long as one is interested in obtaining the corrections near the classical transition, the approximation is justified and $\delta\sigma_{sh}^{AL}$ is indeed the dominant contribution. We will show below that in this limit, the result we obtain is in agreement with the existing literature.[6] In the $\alpha \ll T \sim T_{c0}$ limit, we can expand

$$\gamma(-i\Omega_1,\mathbf{q}) \to \frac{\mathbf{q}}{2\pi T}\psi'\left(\frac{1}{2}\right)+\frac{\alpha_q-i\Omega_1/2}{2\pi T}\psi''\left(\frac{1}{2}\right), \tag{48}$$

where we have used $\Omega_1 \ll T$, in addition. Keeping the zeroth order term amounts to making the static approximation ($\Omega_1=0$) and Eq. (45) reduces to

$$\delta\sigma_{sh}^{AL} = \frac{2}{d}\frac{D^2e^2}{(2\pi T)^3}\psi'\left(\frac{1}{2}\right)^2\int\frac{d^dq}{(2\pi)^d}\frac{d\Omega_1}{\sinh^2\frac{\Omega_1}{2T}}q^2 \times[\mathrm{Im}\,K(-i\Omega_1,q)]^2. \tag{49}$$

Using Eq. (30) for the fluctuation propagator in the limit under consideration, we have

$$\mathrm{Im}\,K(-i\Omega_1,q) = \frac{4\pi T}{\psi'(1/2)}\frac{\Omega_1}{(\tilde{\delta}_T+Dq^2)^2+\Omega_1^2}, \tag{50}$$

where

$$\tilde{\delta}_T = \delta_T(0,T)\frac{4\pi T}{\psi'(1/2)}. \tag{51}$$

Further, using $\sinh x \to x$ for small x, we can write the final expression as

$$\delta\sigma_{sh}^{AL} = \frac{16TD^2e^2}{\pi d}\int\frac{d^dqd\Omega_1}{(2\pi)^d}\frac{q^2}{[(\tilde{\delta}_T+Dq^2)^2+\Omega_1^2]^2} = \frac{D^2e^2}{T^2}\int\frac{d^dq}{d(2\pi)^d}\frac{q^2}{\left(\tilde{\tilde{\delta}}_T+\frac{Dq^2}{2T}\right)^3}, \tag{52}$$

where we have redefined

$$\tilde{\tilde{\delta}}_T = \frac{4\delta_T(0,T)}{\pi} = \frac{\tilde{\delta}_T}{2T} \tag{53}$$

to put the integral in a form similar to what we will find in one of the regimes near the quantum phase transition. The presentation of the results for different dimensions will accordingly be deferred to Sec. IV in order to facilitate the comparison.

Now, we move on to the other two corrections given by the density-of-states and the Maki-Thompson diagrams, as shown in Fig. 2. The calculation follows on lines similar to what we have outlined for the case of the Aslamazov-Larkin diagram in detail above. We find that the density-of-state fluctuation correction can be expressed as

$$\delta\sigma^{DOS} = \delta\sigma_{sh}^{DOS}+\delta\sigma_{cth}^{DOS}, \tag{54}$$

where

$$\delta\sigma_{sh}^{DOS} = \frac{D^2e^2}{4\pi T}\int\frac{d^dqd\omega d\Omega}{(2\pi)^d}\tanh\frac{\omega}{2T}\frac{iK(-i\Omega,q)}{\sinh^2\frac{\Omega}{2T}} \times\left[-\mathrm{Re}\,\frac{1}{(\alpha_q-i\omega_+)^2}+\mathrm{Re}\,\frac{q_x^2}{(\alpha_q-i\omega_+)^3}\right] \tag{55}$$

and

$$\delta\sigma_{cth}^{DOS} = -A+\frac{3}{2}B, \tag{56}$$

with

$$A = -\frac{De^2}{2\pi}\int\frac{d^dqd\omega d\Omega}{(2\pi)^d}\tanh\frac{\omega}{2T}\coth\frac{\Omega}{2T} \times\left[\frac{1}{(\alpha_q-i\omega_+)^3}K(-i\Omega,q)\right] \tag{57}$$

and

$$B = -\frac{De^2}{2\pi}\int\frac{d^dqd\omega d\Omega}{(2\pi)^d}\tanh\frac{\omega}{2T}\coth\frac{\Omega}{2T} \times\left[\frac{q_x^2}{(\alpha_q-i\omega_+)^4}K(-i\Omega,q)\right]. \tag{58}$$

Here,

$$\omega_+ \equiv \omega+\Omega/2, \tag{59}$$

and A and B are introduced for future convenience. The first term in each of $\delta\sigma_{sh}^{DOS}$ and $\delta\sigma_{cth}^{DOS}$ comes from the evaluation of the first two density-of-states diagrams, while the second term comes from the density-of-states diagram that contains an extra Cooperon.

The Maki-Thompson correction can be expressed as

$$\delta\sigma^{MT} = \delta\sigma_{sh}^{MT}+\delta\sigma_{cth}^{MT}, \tag{60}$$

where

$$\delta\sigma_{sh}^{MT} = \frac{D^2e^2}{4\pi T}\int \frac{d^dqd\omega d\Omega}{(2\pi)^d}\tanh\frac{\omega}{2T}\frac{iK(-i\Omega,q)}{\sinh^2\dfrac{\Omega}{2T}}\left[\frac{1}{\alpha_q^2+\omega_+^2}\right], \tag{61}$$

while

$$\delta\sigma_{cth}^{MT} = -A + 3B, \tag{62}$$

with A and B defined above. The contribution $\delta\sigma_{sh}^{MT}$ as well as the first term in $\delta\sigma_{cth}^{MT}$ are obtained by evaluating the first of the two Maki-Thompson diagrams. The evaluation of the second diagram with an extra Cooperon yields the second term in $\delta\sigma_{cth}^{MT}$ which is of the same order at low temperatures and of lower order at higher temperatures.

IV. TRANSPORT NEAR THE QUANTUM PHASE TRANSITION

In the previous section, we have derived the expressions for the different fluctuation corrections to the conductivity that are valid in the vicinity of the entire boundary [Eq. (20)] between the superconducting and normal phases in the α-T phase diagram. As the pair-breaking strength is increased, superconductivity breaks down even at $T=0$ once α becomes equal to $\alpha_{c0} \equiv \alpha_c(T=0) = \pi T_{c0}/2\gamma$. In this section, we want to map out the superconducting fluctuation regimes and obtain the finite-temperature crossovers that would appear in the region

$$T \ll \alpha_c(T),$$

$$\alpha - \alpha_c(T) \ll \alpha_c(T), \tag{63}$$

near the pair-breaking quantum phase transition. Note, however, that the validity of our zero-temperature results will not be restricted to the immediate neighborhood of α_{c0}.

A. Dominant fluctuation corrections

Since in this section we are interested in the region delineated by Eq. (63), we will use the asymptotic form of the digamma function

$$\psi\left(\frac{1}{2}+\frac{\alpha_q - i\Omega_1/2}{2\pi T}\right) \to \ln\left(\frac{\alpha_q - i\Omega_1/2}{2\pi T}\right) \tag{64}$$

in the forthcoming treatment. Let us begin by analyzing the Aslamazov-Larkin correction. Using Eq. (64) inside the expression for γ as defined by Eq. (47), we obtain a reduced form

$$\gamma(-i\Omega_1,\mathbf{q}) \to \frac{\mathbf{q}}{\alpha_q - i\Omega_1/2} \to \frac{\mathbf{q}}{\alpha_c(T)}, \tag{65}$$

where the second limit is justified *a posteriori* by the behavior of the integral below. We have

$$\delta\sigma_{sh}^{AL} = \frac{D^2e^2}{\pi T d\alpha_c^2}\int \frac{d^dq}{(2\pi)^d}\frac{d\Omega_1}{\sinh^2\dfrac{\Omega_1}{2T}}q^2[\mathrm{Im}\,K(-i\Omega_1,q)]^2, \tag{66}$$

where

$$\mathrm{Im}\,K(-i\Omega_1,q) = \frac{\Omega_1/[2\alpha_c(T)]}{\left[\delta_\alpha(\alpha,T)+\dfrac{Dq^2}{2\alpha_c(T)}\right]^2+\left[\dfrac{\Omega_1}{2\alpha_c(T)}\right]^2} \tag{67}$$

is obtained using Eq. (32). Indeed, the integral is dominated by small values of q and Ω_1 and $\delta\sigma_{sh}^{AL}$ is critical in the vicinity of $\alpha_c(T)$. That is also the reason why it was legitimate to use the reduced form for K.

At this point, the reader should observe that to analytically analyze $\delta\sigma_{sh}^{AL}$ any further, we need to order the energy scales, T and $\alpha-\alpha_c(T)$. The frequency integral can then be carried out to get the limiting form

$$\delta\sigma_{<,sh}^{AL} = \frac{2\pi}{3}\frac{D^2e^2T^2}{\alpha_c^4}\int \frac{d^dq}{d(2\pi)^d}\frac{q^2}{\left[\delta_\alpha(\alpha,T)+\dfrac{Dq^2}{2\alpha_c(T)}\right]^4} \tag{68}$$

for $T \ll \alpha-\alpha_c(T)$ and

$$\delta\sigma_{>,sh}^{AL} = \frac{D^2e^2T}{\alpha_c^3}\int \frac{d^dq}{d(2\pi)^d}\frac{q^2}{\left[\delta_\alpha(\alpha,T)+\dfrac{Dq^2}{2\alpha_c(T)}\right]^3} \tag{69}$$

for $T \gg \alpha-\alpha_c(T)$. Observe that the integrand in Eq. (69) has exactly the same form as the integrand in Eq. (52) corresponding to the Aslamazov-Larkin correction in the temperature vicinity above the classical transition at T_{c0} in the absence of any pair-breaking perturbation. Whereas $\delta_T(0,T)$ and T were the parameters in that integrand, here they are $\delta_\alpha(\alpha,T)$ and $\alpha_c(T)$ instead.

To be able to access the crossover between the two limiting forms, $\delta\sigma_{<,sh}^{AL}$ and $\delta\sigma_{>,sh}^{AL}$, we recast Eq. (66) in terms of dimensionless variables to obtain

$$\delta\sigma_{sh}^{AL} = \frac{2D^2e^2}{\pi dT^2}\left(\frac{2T}{D}\right)^{(2+d)/2}F(\eta), \tag{70}$$

where

$$F(\eta) = \int \frac{d^dq}{(2\pi)^d}\frac{d\Omega_1}{\sinh^2\Omega_1}\frac{q^2\Omega_1^2}{[(\eta+q^2)^2+{\Omega_1}^2]^2} \tag{71}$$

is a scaling function of the dimensionless parameter

$$\eta \equiv \frac{\alpha-\alpha_c(T)}{T}. \tag{72}$$

In the $\eta \gg 1$ limit, $\delta\sigma_{sh}^{AL}$ reduces to Eq. (68), while in the $\eta \ll 1$ limit, it reduces to Eq. (69). The numerical evaluation of $F(\eta)$ gives the behavior $\delta\sigma_{sh}^{AL}$ over the entire range of η.

Now, let us proceed to analyze the $\delta\sigma_{cth}^{AL}$ part of the Aslamazov-Larkin correction. After using the asymptotic form of the digamma function given by Eq. (64) to get a simplified expression, we express $\delta\sigma_{cth}^{AL}$ as a sum of two terms:

$$\delta\sigma_{cth}^{AL} = \frac{D^2e^2}{\pi i}\int \frac{d^dq d\Omega_1}{(2\pi)^d}\frac{q_x^2K^2(-i\Omega_1,q)}{(\alpha_q - i\Omega_1/2)^3} \times\left[\left(\coth\frac{\Omega_1}{2T} - \mathrm{sign}\frac{\Omega_1}{2T}\right) + \mathrm{sign}\frac{\Omega_1}{2\mathrm{T}}\right]. \quad (73)$$

At any finite temperature, the first (difference) term can be shown to be subdominant as compared to $\delta\sigma_{sh}^{AL}$ while for $T=0$, it vanishes identically. Thus, we need evaluate only the second term which is independent of temperature. To this end, we carry out a bunch of manipulations and do the frequency integration by parts to obtain a neat expression which we denote by

$$\delta\sigma_{0,cth}^{AL} = \frac{4De^2}{\pi d(d+2)}\int \frac{d^dq}{(2\pi)^d}\frac{(Dq^2)^2K^2(0,q)}{\alpha_q^3}. \quad (74)$$

As for the Maki-Thompson and the density-of-states corrections, we find that $\delta\sigma_{sh}^{DOS}+\delta\sigma_{sh}^{MT}$ is subdominant as compared to the Aslamazov-Larkin correction $\delta\sigma_{sh}^{AL}$. On the other hand, the same way as we did in Eq. (73), we can express $\delta\sigma_{cth}^{DOS}$ and $\delta\sigma_{cth}^{MT}$ as a sum of a temperature-dependent term that vanishes at $T=0$ and a second temperature-independent term. The temperature-dependent term is again subdominant as compared to $\delta\sigma_{sh}^{AL}$, and after some manipulation, we find the temperature-independent part of A and B [see Eqs. (57) and (58)] to be given by

$$A_0 = \frac{2De^2}{\pi}\int \frac{d^dq}{d(2\pi)^d}\frac{Dq^2K(0,q)}{\alpha_q^2} \quad (75)$$

and

$$B_0 = \frac{4De^2}{3\pi}\int \frac{d^dq}{d(d+2)(2\pi)^d}\frac{(Dq^2)^2K(0,q)}{\alpha_q^3}. \quad (76)$$

We can reexpress B_0 as

$$B_0 = \frac{A_0}{3} - \tilde{B}_0, \quad (77)$$

$$\tilde{B}_0 = \frac{2De^2}{3\pi d(d+2)}\int \frac{d^dq}{(2\pi)^d}\frac{(Dq^2)^2K^2(0,q)}{\alpha_q^3} \quad (78)$$

such that we have

$$\delta\sigma_{0,cth}^{AL} = 6\tilde{B}_0, \quad (79)$$

$$\delta\sigma_{0,cth}^{DOS} = -\frac{A_0+3\tilde{B}_0}{2}, \quad (80)$$

$$\delta\sigma_{0,cth}^{MT} = -3\tilde{B}_0 \quad (81)$$

to yield

$$\delta\sigma_{0,cth} \equiv \delta\sigma_{0,cth}^{AL} + \delta\sigma_{0,cth}^{DOS} + \delta\sigma_{0,cth}^{MT} = -\frac{A_0-3\tilde{B}_0}{2} = -\frac{3B_0}{2} = \frac{-2De^2}{\pi}\int \frac{d^dq}{d(d+2)(2\pi)^d}\frac{(Dq^2)^2K(0,q)}{\alpha_q^3}, \quad (82)$$

where A_0, B_0, and $\tilde{B}_0$ are all positive quantities defined above. The expression for $K(0,q)$ is given by Eq. (31) which is appropriate for $T \ll \alpha_{c0}$.

B. Fluctuation regimes in the α-T plane

In the previous subsection, we have identified and analyzed the dominant fluctuation corrections to the normal state conductivity in the vicinity of a pair-breaking quantum phase transition out of a superconducting state. Based on this analysis, the fluctuation conductivity is

$$\delta\sigma(\alpha,T) = \delta\sigma_{0,cth}(\alpha) + \delta\sigma_{sh}^{AL}(\alpha,T), \quad (83)$$

where $\delta\sigma_{0,cth}(\alpha)$ is given by Eq. (82) and $\delta\sigma_{sh}^{AL}(\alpha,T)$ is given by Eq. (66). At the absolute zero of the temperature, the correction to the conductivity is given by

$$\delta\sigma(\alpha,0) = \delta\sigma_{0,cth}(\alpha), \quad (84)$$

and it continues to be the dominant correction up to a temperature scale $T_0(\alpha)$ at which $\delta\sigma_{sh}^{AL}(\alpha,T)$ becomes comparable. This regime with a negative fluctuation correction which turns out to be almost noncritical is the "quantum regime" with thermal fluctuations playing no role whatsoever. In this regime, the Maki-Thompson correction turns out to be negative and is half the magnitude of the positive Aslamazov-Larkin correction; the negative density-of-states correction too is of the same order, and the total is negative. The presence of the superconducting fluctuations thus impedes the flow of current, contrary to the naive expectation. It is important to note that the quantum regime is outside the scope of any theoretical approach that does not take into account the electron degrees of freedom in addition to the superconducting fluctuations.

On the other hand, the regime defined by $T > \alpha - \alpha_c(T)$ is dominated by the Aslamazov-Larkin correction $\delta\sigma_{sh}^{AL}$ in its limiting form $\delta\sigma_{>,sh}^{AL}$ given by Eq. (69); this is the "classical regime." The "intermediate regime" in between the classical and quantum regimes is dominated by $\delta\sigma_{<,sh}^{DOS}$, which is the limiting form of the Aslamazov-Larkin correction appropriate for $T \ll \alpha - \alpha_c(T)$, and is given by Eq. (68). The fluctuation conductivity in both the classical and the intermediate regime enhances the normal state conductivity due to the additional channel of transport via the fluctuating Cooper pairs and is more critical than that in the quantum regime.

The presence of these three regimes (see Fig. 3) means that the conductivity behavior depends on how the quantum phase transition or the low-temperature transition is approached. If the quantum critical point is approached by lowering the temperature at a fixed value of $\alpha = \alpha_{c0}$, then the measurement trajectory sweeps exclusively across the classical regime and diverges as the temperature tends to zero. On

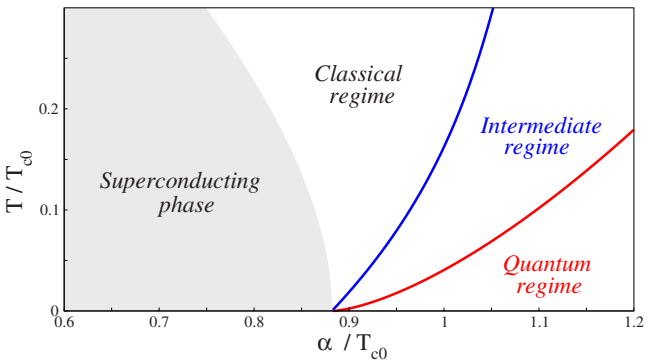

FIG. 3. (Color online) Phase diagram showing the vicinity of the superconducting quantum critical point realized via a pair-breaking quantum phase transition as illustrated in Fig. 1. The boundary between the classical and the intermediate regime is given by $T=\alpha-\alpha_c(T)$. The analytical estimate for the boundary between quantum and intermediate regimes is given by Eqs. (94), (104), and (113) for the case of a nanowire or doubly connected cylinder, a thin film, and a bulk superconductor, respectively. For clarity, only the case of $d=1$ is shown. The quantum regime extends to higher temperatures as the effective dimensionality of the system is increased.

the other hand, if α_{c0} is approached by tuning the pair-breaking parameter at a fixed value of $T=0$, then the path lies entirely in the quantum regime showing the characteristic increase in resistance. On the contrary, going away from α_{c0} results in a decrease in the resistance as α is increased; if the pair-breaking strength were to be tuned by a parallel magnetic field, a negative magnetoresistance is observed. The intermediate regime is swept only while the measurement trajectory crosses over from the quantum to the classical regime or vice versa. A trajectory in which the temperature is varied at a fixed value of $\alpha>\alpha_{c0}$ or α is tuned at a nonzero temperature results in a nontrivial conductivity with a nonmonotonic behavior.

1. Nanowire or doubly connected cylinder ($d=1$)

Consider a pair-breaking quantum phase transition in a superconducting nanowire driven by tuning a magnetic field, the concentration of magnetic impurities, or yet another pair-breaking perturbation. As long as the diameter of the wire is smaller than the superconducting coherence length, the system is effectively one dimensional as far as superconducting fluctuations are concerned. One could also consider a doubly connected cylinder instead of a wire, as discussed in Sec. II.

For $d=1$, the fluctuation conductivity in the classical regime $[T>\alpha-\alpha_c(T)]$, given by Eq. (69), can be written in terms of a dimensionless integral to obtain

$$\delta\sigma^{AL}_{>,sh}(\alpha,T)=\frac{\sqrt{D}e^2T}{2\pi\alpha_c^{3/2}}\int_{-\infty}^{\infty}dx\frac{x^2}{[\delta_\alpha(\alpha,T)+x^2/2]^3}$$
$$=\frac{\sqrt{D}e^2}{4\sqrt{2}}\frac{T}{[\alpha-\alpha_c(T)]^{3/2}}. \tag{85}$$

The temperature dependence is more revealing if one uses $\alpha_c(T)\sim\alpha_{c0}-\pi^2T^2/(6\alpha_{c0})$ in the vicinity of α_{c0} [see Eq. (22)]. In particular, if the quantum critical point at α_{c0} is approached by lowering the temperature, then

$$\delta\sigma^{AL}_{>,sh}(\alpha_{c0},T)=\frac{3\sqrt{3}\sqrt{D}e^2}{2\pi^3}\frac{\alpha_{c0}^{3/2}}{T^2} \tag{86}$$

shows a quantum critical divergence with the power T^{-2} when $T\to0$.

It is instructive to compare the result in Eq. (85) in the classical regime with the fluctuation conductivity

$$\delta\sigma^{AL}_{sh}(0,T)=\frac{\pi\sqrt{\pi}\sqrt{D}e^2}{32\sqrt{2}}\frac{T_{c0}}{(T-T_{c0})^{3/2}} \tag{87}$$

in the temperature vicinity above the classical transition at T_{c0} in the absence of any pair-breaking perturbation. Derivation of this result requires evaluating Eq. (52) which contains the same dimensionless integral as in the classical regime near the quantum phase transition.

By using Eq. (68), we have

$$\delta\sigma^{AL}_{<,sh}(\alpha,T)=\frac{\sqrt{D}T^2e^2}{3\alpha_c^{5/2}}\int_{-\infty}^{\infty}dx\frac{x^2}{[\delta_\alpha(\alpha,T)+x^2/2]^4}$$
$$=\frac{\pi\sqrt{D}e^2}{12\sqrt{2}}\frac{T^2}{[\alpha-\alpha_c(T)]^{5/2}} \tag{88}$$

in the intermediate regime between the classical and quantum regimes. The fluctuation conductivity contains an additional power of $T/[\alpha-\alpha_c(T)]$ as compared to the classical regime.

Expressed in terms on the scaling function that we introduced in Eq. (70), we have

$$\delta\sigma^{AL}_{sh}(\alpha,T)=\frac{4\sqrt{2}\sqrt{D}e^2}{\pi\sqrt{T}}F(\eta), \tag{89}$$

with

$$F(\eta)=\begin{cases}\dfrac{\pi}{32}\eta^{-3/2}, & \eta\ll1\\ \dfrac{\pi^2}{96}\eta^{-5/2}, & \eta\gg1,\end{cases} \tag{90}$$

where η is defined in Eq. (72). The full scaling function given by Eq. (71) and the negative temperature-independent term $\delta\sigma_{0,cth}(\alpha)$, as discussed below, can be evaluated numerically. In this way, we are able to get the behavior of the fluctuation conductivity as a function of temperature and pair-breaking parameter, in the entire neighborhood of the superconducting quantum critical point. The exact boundary of the quantum regime in the α-T phase diagram can then be identified by tracing the curve on which the fluctuation conductivity becomes zero while changing sign from positive to negative.

The temperature-independent fluctuation correction which dominates the quantum regime is given by evaluating Eq. (82) to obtain

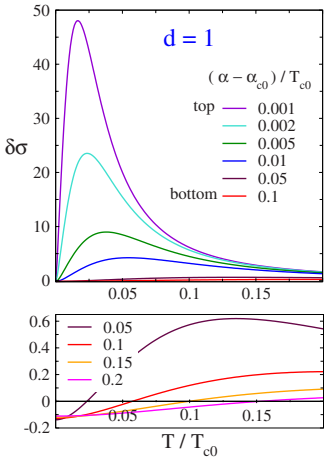

FIG. 4. (Color online) Temperature dependence of the fluctuation correction to the conductivity (in units of $\sqrt{D}e^2$) in the vicinity of a pair-breaking quantum phase transition at $\alpha=\alpha_{c0}=0.889T_{c0}$ for $d=1$ (nanowire or doubly connected cylinder). Plots are shown for different values of $(\alpha-\alpha_{c0})/T_{c0}$. When the superconducting QCP is approached by lowering the temperature at $\alpha=\alpha_{c0}$, the quantum critical divergence of the conductivity is given by Eq. (86) (not included in the figure). The lower panel clearly displays the temperatures $T_0(\alpha)$ [analytically estimated by Eq. (94)], at which the correction becomes negative, thereby signaling the entry into the quantum regime at a given value of α.

$$\delta\sigma_{0,cth}(\alpha) = -\frac{\sqrt{D}e^2}{3\pi^2\sqrt{\alpha_{c0}}}\int_{-\infty}^{\infty} dx \frac{x^4}{h_\alpha(x)^3 \ln h_\alpha(x)}, \quad (91)$$

where

$$h_\alpha(x) \equiv 1 + \delta_\alpha(\alpha,0) + x^2/2. \quad (92)$$

The correction has no critical divergence at $\alpha=\alpha_{c0}$ [i.e., $\delta_\alpha(\alpha,0)=0$] and even the first derivative is noncritical. The second derivative diverges as $(\alpha-\alpha_{c0})^{-1/2}$, thereby giving the first nonanalytic term in the expansion (obtained by integrating twice) around α_{c0}. We thus obtain

$$\delta\sigma_{0,cth}(\alpha) - \delta\sigma_{0,cth}(\alpha_{c0}) = \frac{e^2\sqrt{D}}{\sqrt{\alpha_{c0}}}[a_1\delta_\alpha(\alpha,0) + b_1\delta_\alpha(\alpha,0)^{3/2} + \cdots], \quad (93)$$

with $a_1=0.386$ and $b_1=-4\sqrt{2}/(3\pi)$. By using the first term in the expansion, one can analytically estimate the boundary between the intermediate and the quantum regimes to be

$$\frac{T_0(\alpha)}{T_{c0}} \sim \left(\frac{\alpha-\alpha_{c0}}{\alpha_{c0}}\right)^{7/4}. \quad (94)$$

In Figs. 4 and 5, we display the plots for the fluctuation conductivity when the vicinity of the pair-breaking quantum phase transition is explored by sweeping either the temperature or the pair-breaking parameter (see the figure captions for details). As discussed above, a quantum critical divergence is expected as temperature is lowered by sitting at $\alpha=\alpha_{c0}$ and is not shown in the figure. If α is increased starting from α_{c0} at a fixed value of $T=0$, the conductivity increases

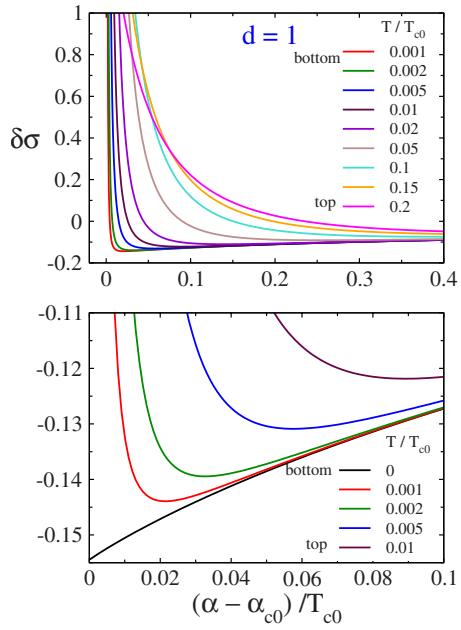

FIG. 5. (Color online) Fluctuation correction to the conductivity (in units of $\sqrt{D}e^2$) in the vicinity of a pair-breaking quantum phase transition at $\alpha_{c0}=0.889T_{c0}$ for $d=1$ (nanowire or doubly connected cylinder). Plots show the behavior of $\delta\sigma$ as one sweeps $(\alpha-\alpha_{c0})/T_{c0}$ at a given value of T/T_{c0}. The lower panel shows the negative correction at $T=0$ and a clear upturn of the conductivity which is characteristic of the quantum regime. This would correspond to a decrease in resistance (a negative magnetoresistance, if α is tuned by a magnetic field) as α is increased at $T=0$ and a clearly visible nonmonotonic behavior at low temperatures.

monotonically, correspondingly giving a decrease in resistance, i.e., a negative magnetoresistance if α is tuned by a magnetic field. The conductivity shows a nonmonotonic behavior as α is varied at a fixed $T\neq 0$ or T is varied at a fixed $\alpha>\alpha_{c0}$, the behavior being more distinct for smaller values of T and $\alpha-\alpha_{c0}$, respectively.

2. Thin film ($d=2$)

Consider a pair-breaking quantum phase transition in a superconducting thin film whose thickness is smaller than the coherence length which makes the system effectively two dimensional as far as superconducting fluctuations are concerned. The transition can be driven, e.g., by tuning a pair-breaking perturbation such as a parallel magnetic field or the concentration of magnetic impurities as discussed in Sec. II.

The remarkable fact about the fluctuation conductivity in two dimensions is that it is a universal quantity, independent of the properties of the material under consideration. The fluctuation conductivity in the classical regime $[T>\alpha-\alpha_c(T)]$, given by Eq. (69), can be evaluated for $d=2$ to obtain

$$\delta\sigma^{AL}_{>,sh}(\alpha,T) = \frac{Te^2}{4\pi\alpha_c}\int_0^\infty dx \frac{x^3}{[\delta_\alpha(\alpha,T)+x^2/2]^3} = \frac{e^2}{4\pi}\frac{T}{\alpha-\alpha_c(T)}, \quad (95)$$

with $\alpha_c(T)\sim\alpha_{c0}-\pi^2T^2/(6\alpha_{c0})$ in the vicinity of α_{c0} [see Eq. (22)]. If the quantum critical point is approached by lowering

the temperature at a fixed $\alpha=\alpha_{c0}$, then we have

$$\delta\sigma^{AL}_{>,sh}(\alpha_{c0},T)=\frac{3e^2}{2\pi^3}\frac{\alpha_{c0}}{T}, \tag{96}$$

which shows a quantum critical divergence T^{-1} when $T\to 0$.

The fluctuation conductivity [Eq. (52)] in the temperature vicinity above the classical transition at T_{c0} in the absence of any pair-breaking perturbation contains the same form of the integrand as in the classical regime near the quantum phase transition, therefore giving a result

$$\delta\sigma^{AL}_{sh}(0,T)=\frac{e^2}{16}\frac{T_{c0}}{T-T_{c0}}, \tag{97}$$

analogous to Eq. (95) and consistent with the classic literature.[6]

By using Eq. (68), the fluctuation conductivity in the intermediate regime is given by

$$\delta\sigma^{AL}_{<,sh}(\alpha,T)=\frac{T^2e^2}{12\alpha_c^2}\int_0^\infty dx\frac{x^3}{[\delta_\alpha(\alpha,T)+x/2]^4}$$
$$=\frac{e^2}{18}\frac{T^2}{[\alpha-\alpha_c(T)]^2}. \tag{98}$$

It contains an additional power of $T/[\alpha-\alpha_c(T)]$ as compared to the classical regime, just as we found for $d=1$. Expressed in terms on the scaling function that we introduced in Eq. (70), we have

$$\delta\sigma^{AL}_{sh}(\alpha,T)=\frac{4e^2}{\pi}F(\eta), \tag{99}$$

with

$$F(\eta)=\begin{cases}\frac{1}{16}\eta^{-1}, & \eta\ll 1\\ \frac{\pi}{72}\eta^{-2}, & \eta\gg 1,\end{cases} \tag{100}$$

and the full form of $F(\eta)$ can be evaluated by doing the integrals in Eq. (71) numerically.

The temperature-independent quantum correction which dictates the behavior in the quantum regime can be obtained by using Eq. (82) to have

$$\delta\sigma_{0,cth}(\alpha)=-\frac{e^2}{8\pi^2}\int_0^\infty dx\frac{x^5}{h_\alpha(x)^3\ln h_\alpha(x)}, \tag{101}$$

where $h_\alpha(x)$ is defined by Eq. (92). For large x, the integrand goes as $1/(x\ln x)$ and the integral has a very weak ultraviolet divergence which can be isolated by evaluating the integral analytically by parts (Λ is the cutoff). Indeed, at $\alpha=\alpha_{c0}$ we find

$$\delta\sigma_{0,cth}(\alpha_{c0})=-\frac{e^2}{2\pi^2}\ln\left(\ln\frac{\Lambda}{2}\right)+\frac{e^2}{4\pi^2}\int_0^\infty dx\frac{x\ln[\ln(1+x/2)]}{(1+x/2)^3}$$
$$=-\frac{e^2}{2\pi^2}\ln\left(\ln\frac{\Lambda}{2b}\right), \tag{102}$$

where $b=1.122\,92$. We can thus consider the difference $\delta\sigma_{0,cth}(\alpha)-\delta\sigma_{0,cth}(\alpha_{c0})$ that has a convergent integral to be evaluated numerically.

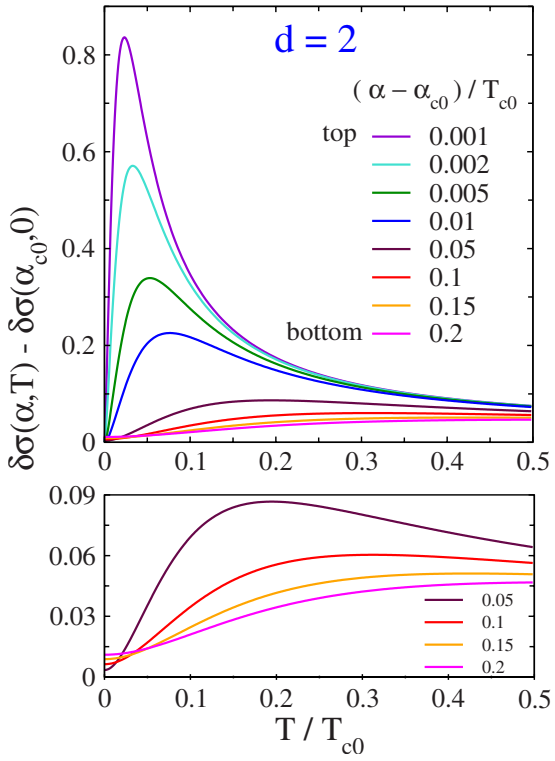

FIG. 6. (Color online) Temperature dependence of the fluctuation correction to the conductivity (in units of e^2) in the vicinity of a pair-breaking quantum phase transition at $\alpha=\alpha_{c0}=0.889T_{c0}$, for the case of a thin film ($d=2$). Plots are shown for different values of $(\alpha-\alpha_{c0})/T_{c0}$. When the superconducting QCP is approached by lowering the temperature at $\alpha=\alpha_{c0}$, the quantum critical divergence of the conductivity is given by Eq. (96) (not included in the figure). Note that we have plotted the difference $\delta\sigma(\alpha,T)-\delta\sigma(\alpha_{c0},0)$ which is always positive given that $\delta\sigma(\alpha,0)$ is most negative at $\alpha=\alpha_{c0}$ (see Fig. 7).

Here again as in the $d=1$ case, $\delta\sigma_{0,cth}(\alpha)$ as well as the first derivative have no critical divergence at $\alpha=\alpha_{c0}$. From the divergence in the second derivative, we can get the first nonanalytic term in the expansion around α_{c0}. We thus have

$$\delta\sigma_{0,cth}(\alpha)-\delta\sigma_{0,cth}(\alpha_{c0})$$
$$=e^2[a_2\delta_\alpha(\alpha,0)+b_2\delta_\alpha(\alpha,0)^2\ln\delta_\alpha(\alpha,0)+\cdots], \tag{103}$$

with $a_2=0.070$ and $b_2=1/(2\pi^2)$. By using the first term in the expansion, one can analytically estimate the boundary between the intermediate and the quantum regimes to be

$$\frac{T_0(\alpha)}{T_{c0}}\sim\left(\frac{\alpha-\alpha_{c0}}{\alpha_{c0}}\right)^{3/2}. \tag{104}$$

In Figs. 6 and 7, we display the plots for the fluctuation conductivity when the vicinity of the pair-breaking quantum phase transition is explored by sweeping either the temperature or the pair-breaking parameter (see figure captions for more details). The behavior of the fluctuation conductivity is

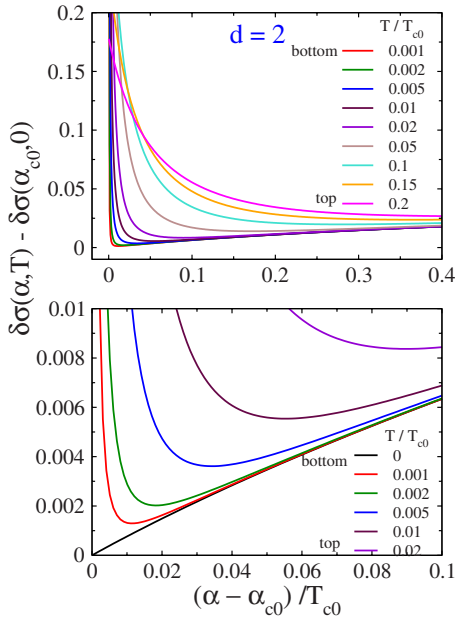

FIG. 7. (Color online) Fluctuation correction to the conductivity (in units of e^2) in the vicinity of a pair-breaking quantum phase transition at $\alpha_{c0}=0.889T_{c0}$ for $d=2$ (thin films). Plots show the behavior of $\delta\sigma(\alpha,T)-\delta\sigma(\alpha_{c0},0)$ as one sweeps $(\alpha-\alpha_{c0})/T_{c0}$ at a given value of T/T_{c0}. The lower panel shows the correction at $T=0$ and a clear upturn of the conductivity which is characteristic of the quantum regime. This would correspond to a decrease in resistance (negative magnetoresistance) as α is increased at $T=0$ and a clearly visible nonmonotonic behavior at low temperatures.

qualitatively similar to the case of $d=1$. However, the critical divergences are weaker and the ratio of the fluctuation correction to the normal state conductivity is expected to be lower as well.

3. Bulk ($d=3$)

Although the pair-breaking quantum phase transition out of a superconducting state in low-dimensional disordered systems attracts more attention, we will now consider such a transition in a three-dimensional bulk superconductor mainly for the sake of comparison and completeness. One could imagine superconductivity at low temperatures being destroyed by magnetic impurities, for example. The discussion below parallels the preceding analysis for $d=1,2$.

The fluctuation conductivity in the classical regime [Eq. (69)] is given by

$$\delta\sigma^{AL}_{>,sh}(\alpha,T)=\frac{Te^2}{6\pi^2\sqrt{D}\sqrt{\alpha_c}}\int_0^\infty dx\frac{x^4}{[\delta_\alpha(\alpha,T)+x^2/2]^3}=\frac{e^2}{4\pi\sqrt{2}\sqrt{D}}\frac{T}{\sqrt{\alpha-\alpha_c(T)}} \tag{105}$$

and at $\alpha=\alpha_{c0}$ reduces to

$$\delta\sigma^{AL}_{>,sh}(\alpha_{c0},T)=\frac{\sqrt{3}e^2\sqrt{\alpha_{c0}}}{\sqrt{D}4\pi^2}, \tag{106}$$

which is independent of temperature. This is in stark contrast to a quantum critical divergence found in the case of one and two dimensions on approaching the quantum phase transition by lowering the temperature. It illustrates the fact that fluctuations are stronger and consequently play a more crucial role in reduced dimensions.

Same as for a nanowire and a thin film, note that the fluctuation conductivity [Eq. (52)] near the classical transition at T_{c0} in the absence of any pair-breaking perturbation is analogous in form to that in the classical regime and is given by

$$\delta\sigma^{AL}_{sh}(0,T)=\frac{e^2}{8\sqrt{2\pi}\sqrt{D}}\frac{T_{c0}}{\sqrt{T-T_{c0}}}. \tag{107}$$

Although it is critical, the divergence is weaker by one power of $(T-T_{c0})^{-1/2}$ as compared to that in two dimensions, which in turn is weaker than that in one dimension by the same power.

By using Eq. (68), the fluctuation conductivity in the intermediate regime is given by

$$\delta\sigma^{AL}_{<,sh}(\alpha,T)=\frac{T^2e^2}{9\pi\sqrt{D}\alpha_c^{3/2}}\int_0^\infty dx\frac{x^4}{[\delta_\alpha(\alpha,T)+x^2/2]^4}=\frac{e^2}{36\sqrt{2}\sqrt{D}}\frac{T^2}{[\alpha-\alpha_c(T)]^{3/2}}. \tag{108}$$

It contains an additional power of $T/[\alpha-\alpha_c(T)]$ as compared to the classical regime, just as we found for $d=1,2$. Alternatively, expressing $\delta\sigma^{AL}_{sh}(\alpha,T)$ in terms on the scaling function that we introduced in Eq. (70), we have

$$\delta\sigma^{AL}_{sh}(\alpha,T)=\frac{8\sqrt{2}e^2\sqrt{T}}{3\pi\sqrt{D}}F(\eta), \tag{109}$$

with

$$F(\eta)=\begin{cases}\frac{3}{64}\eta^{-1/2}, & \eta\ll 1\\ \frac{\pi}{192}\eta^{-3/2}, & \eta\gg 1,\end{cases} \tag{110}$$

and the full form of $F(\eta)$ can be evaluated by doing the integrals in Eq. (71) numerically.

The temperature-independent quantum correction which dictates the behavior in the quantum regime can be obtained by using Eq. (82) to have

$$\delta\sigma_{0,cth}(\alpha)=-\frac{e^2\sqrt{\alpha_{c0}}}{15\pi^3\sqrt{D}}\int_0^\infty dx\frac{x^6}{h_\alpha(x)^3\ln h_\alpha(x)}, \tag{111}$$

where $h_\alpha(x)$ is defined by Eq. (92). The integral can again be regulated by considering the difference $\delta\sigma_{0,cth}(\alpha)-\delta\sigma_{0,cth}(\alpha_{c0})$ as we did in the case of $d=2$, and can then be subjected to numerical evaluation.

By following the same procedure in one and two dimensions, we get the expansion

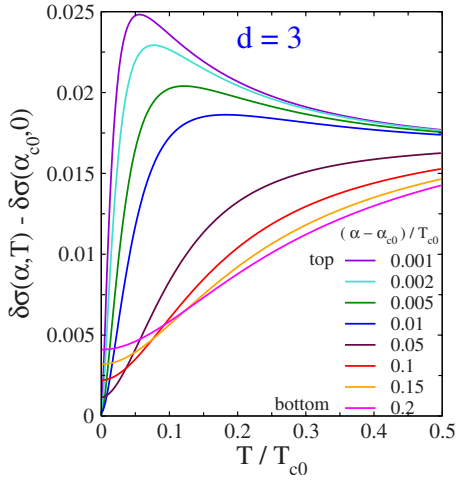

FIG. 8. (Color online) Temperature dependence of the fluctuation correction to the conductivity (in units of $e^2/\sqrt{D}$) in the vicinity of a pair-breaking quantum phase transition at $\alpha_{c0}=0.889T_{c0}$, for the case of a bulk system ($d=3$). Plots are shown for different values of $(\alpha-\alpha_{c0})/T_{c0}$. When the superconducting QCP is approached by lowering the temperature at $\alpha=\alpha_{c0}$, there is no quantum critical divergence of the conductivity, in contrast to what is found for $d=1,2$ and, in fact, the conductivity is temperature independent [see Eq. (106)]. Note that we have plotted the difference $\delta\sigma(\alpha,T)-\delta\sigma(\alpha_{c0},0)$ which is always positive given that $\delta\sigma(\alpha,0)$ is most negative at $\alpha=\alpha_{c0}$ (see Fig. 9).

$$\delta\sigma_{0,cth}(\alpha)-\delta\sigma_{0,cth}(\alpha_{c0}) = \frac{e^2\sqrt{\alpha_{c0}}}{\sqrt{D}}[a_3\delta_\alpha(\alpha,0)+b_3\delta_\alpha(\alpha,0)^2+c_3\delta_\alpha(\alpha,0)^{5/2}+\cdots], \tag{112}$$

with $a_3=0.023$, $b_3=-0.061$, and $c_3=4\sqrt{2}/(15\pi^2)$. Note that the critical divergence shows up for the first time in the third derivative to give the first nonanalytic term in the expansion. By using the first term in the expansion, one can make a rough estimate of the boundary between the intermediate and the quantum regimes to be

$$\frac{T_0(\alpha)}{T_{c0}}\sim\left(\frac{\alpha-\alpha_{c0}}{\alpha_{c0}}\right)^{5/4}. \tag{113}$$

The quantum regime is thus expected to extend up to higher temperatures as compared to the case of $d=1,2$. The fluctuation conductivity, however, has a weaker critical divergence as compared to lower dimensions as was found above also for the classical and intermediate regimes.

In Figs. 8 and 9, we display the plots for the fluctuation conductivity when the vicinity of the pair-breaking quantum phase transition is explored by sweeping either the temperature or the pair-breaking parameter. The qualitative behavior is similar to that discussed for the case of one and two dimensions, but the critical divergences are clearly much weaker. The biggest difference in the behavior can be seen if the quantum phase transition at α_{c0} is approached by lowering the temperature: as shown above, there is absolutely no quantum critical divergence and the correction is independent of temperature.

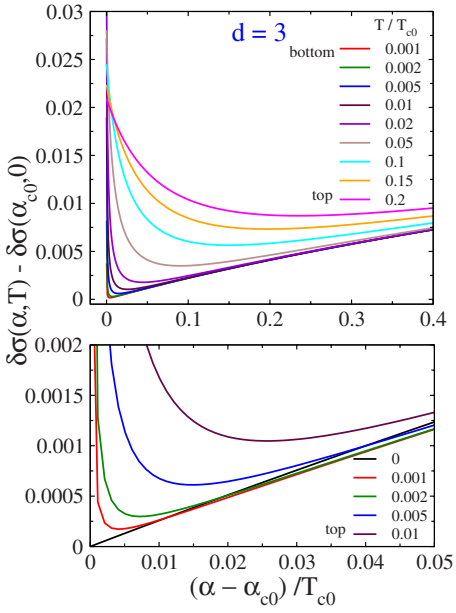

FIG. 9. (Color online) Fluctuation correction to the conductivity (in units of $e^2/\sqrt{D}$) in the vicinity of a pair-breaking quantum phase transition at $\alpha_{c0}=0.889T_{c0}$ for $d=3$ (bulk superconductors). Plots show the behavior of $\delta\sigma(\alpha,T)-\delta\sigma(\alpha_{c0},0)$ as one sweeps $(\alpha-\alpha_{c0})/T_{c0}$ at a given value of T/T_{c0}. The lower panel shows the correction at $T=0$ and a clear upturn of the conductivity which is characteristic of the quantum regime. This would correspond to a decrease in resistance (negative magnetoresistance) as α is increased at $T=0$ and a clearly visible nonmonotonic behavior at low temperatures.

V. RELATED WORK, EXPERIMENTS, AND CONCLUSION

In our work, we have studied the superconducting fluctuation corrections to the normal state conductivity in the entire α-T plane, where α parametrizes the strength of a pair-breaking perturbation, caused by the presence of magnetic impurities or a magnetic field, for example. We have been particularly interested in mapping out the fluctuation regimes in the neighborhood of the pair-breaking quantum phase transition from superconducting to normal state. Our entire analysis has been carried out within the framework of temperature diagrammatic perturbation theory suitable for dirty superconductors and disordered systems.

There have been two previous works which have used an approach different from ours. Ramazashvili and Coleman[20] have used an effective action for the pairing field and evaluated the Aslamazov-Larkin correction to the conductivity using a renormalization group analysis.[21] They have focused on the quantum phase transition driven by magnetic impurities in two and three dimensions for weak (BCS) as well as strong coupling superconductors and derived the behavior of the conductivity when the quantum critical point is approached by lowering the temperature. The temperature de-

pendence matches with what we obtain is two dimensions [see Eq. (96)], but in three dimensions our answers do not match. While they have considered only the "classical renormalization region," Mineev and Sigrist[22] have investigated the entire region around the quantum phase transition using an analogous starting point based on the time-dependent Ginzburg-Landau equations (justifying the use based on arguments by Herbut[23]). They suggest pressure as a tuning parameter, consider weak coupling superconductors in one, two, and three dimensions, and obtain the conductivity corrections in what they call "classical" and "quantum" regimes. Their classical regime is identical to ours, while the answers they find in their quantum regime correspond to our intermediate regime.

The above-mentioned approaches based on using the time-dependent Ginzburg-Landau equations with a linear dissipative time derivative or the corresponding effective action are quite powerful and analogous approaches have proved extremely useful in the study of quantum critical phenomena.[2,21,24] However, the Maki-Thompson and the density-of-states corrections that require the electrons to be present in the theory are outside the scope of these approaches and a microscopic calculation, as we have carried out here, becomes essential to analyze the role of these corrections. Even the zero-temperature Aslamazov-Larkin correction that we find is missed in the effective approaches. On the other hand, our analysis is able to identify the regimes where the contributions involving the interplay between the fluctuating Cooper pairs and the electrons are subdominant, thereby validating the use of the aforementioned effective approaches in those regimes.

We want to mention now some works which also follow a microscopic approach, but for physical configurations different from ours. Beloborodov *et al.*[25,26] have proposed the negative magnetoresistance observed in granular metals in a strong magnetic field and low temperatures to be originating from superconducting fluctuation corrections to the conductivity. Galitski and Larkin[27] have considered two-dimensional superconductors in the presence of a perpendicular magnetic field and again carried out a microscopic analysis of fluctuation corrections taking into account all the diagrams; they too find zero-temperature negative magnetoresistance. As we have discussed in Ref. 28, negative magnetoresistance is found also for a thin film in a parallel instead of perpendicular magnetic field. We think that it is quite a remarkable fact that a negative magnetoresistance at zero temperature is a common feature of all these theories: the Aslamazov-Larkin correction which is always positive, the density-of states correction which is always negative, and the Maki-Thompson correction which has no prescribed sign conspire in all three theories to add up into a total negative correction. Although there might be different reasons for getting a negative correction and a corresponding negative magnetoresistance, it raises the question of whether this is a universal feature of at least a certain class of disordered systems in the presence of a magnetic field and/or pair-breaking perturbation, with fundamental reasons at its heart.

In our work, we have considered the corrections to the conductivity coming into effect due to the proximity of a superconducting state in the low-temperature phase diagram of disordered systems. It is important for our analysis that the disordered conductors under consideration are assumed to be in the metallic (as against insulating) conduction domain. The fact that quantum corrections coming from weak localization effects[13] and electron-electron interactions (the so-called Altshuler-Aronov[14] corrections) significantly modify the conductivity from its Drude-like behavior, even in this domain, does not invalidate our analysis. However, in comparing our theory with experiments, these corrections should be simultaneously taken into account. The weak localization of electron waves is a result of an enhanced backscattering originating from the interference between forward and backward electron trajectories tracing the same path during the course of multiple scattering events. It gives rise to a negative quantum correction to the conductivity, given by the expression[13]

$$\delta\sigma_{WL} = -\frac{2e^2D}{\pi}\int \frac{d^dq}{(2\pi)^d}C(0,q). \tag{114}$$

As is evident from the presence of a Cooperon propagator [Eq. (26)], the interference effects are strongly diminished by the presence of time-reversal symmetry breaking perturbations, thereby yielding a decrease in resistance (a negative magnetoresistance, yet again). On the other hand, the Altshuler-Aronov correction is determined by the diagrams that include only the diffuson propagators and are not sensitive to the magnetic field or other time-reversal symmetry breaking perturbations. Thus, the inclusion of additional quantum corrections will not affect the predicted negative sign of the magnetoresistance (or the decrease of resistance with increasing pair-breaking strength, in the general case) at low temperatures.

The experimental effort in superconducting thin films has so far been motivated to a large extent by interest in the so-called superconductor-insulator transition (SIT),[29] driven by tuning either the disorder (achieved by varying the film thickness) or a perpendicular magnetic field. Questions raised by recent experiments about the mechanism and interpretation of the transition have revived interest also from the theoretical side. Experiments on thin films, observing a suppression of superconductivity in the presence of a perpendicular magnetic field at low temperatures, have conventionally been interpreted within the framework of the field-induced dual-SIT (acronym we will use to refer to a theory based on the boson-vortex duality in a "dirty boson" model,[30] although in the literature such a theory is implicitly implied whenever the acronym SIT is used) mainly based on the negative temperature derivative of the resistance above the critical field and finite size scaling analysis of the data. Gantmakher *et al.*[31] have made the case that a stringent analysis of many of these data sets might point toward inadequacies in such an interpretation. For instance, the phase interpreted as insulating could very well be a metal with quantum corrections, and existence of scaling in a limited region might not be sufficient. To address these points, they have made measurements on NdCeCuO films and found that the microscopic theory based on quantum corrections including the superconducting fluctuation corrections as obtained

by Galitski and Larkin[27] could qualitatively describe the main features of their experiment including the negative magnetoresistance (see the discussion in preceding paragraphs). A possible crossover between the two interpretations is also suggested. Subsequently, Baturina *et al.*[32] have made measurements of magnetic-field-dependent resistance of ultrathin superconducting TiN films with different degrees of disorder and again concluded that the scaling analysis previously regarded as the main evidence of field-induced dual-SIT can, in fact, be observed also for transition from a superconductor to a normal metal with quantum corrections.

The natural question to ask is what happens when superconductivity at very low temperatures is destroyed by applying not a perpendicular but instead a parallel magnetic field for which the field-tuned dual-SIT scenario does not apply. Although there is an interesting set of experiments studying the first order spin paramagnetic transition (e.g., Ref. 33), the case of relevance to us is that of a second order transition. Based on their measurements on InO films with variable oxygen content, Gantmakher *et al.*[34] concluded that the behavior in the parallel and in the perpendicular field-tuned case are very similar. The nonmonotonic magnetoresistance they find in both cases is interesting given that we theoretically find a similar behavior in the case of a parallel magnetic field, as presented in the previous section. Parendo *et al.*[35] have carried out an experiment on ultrathin bismuth films to study the thickness-tuned SIT but in the presence of a parallel magnetic field. In the immediate vicinity of the transition, what they find is a negative magnetoresistance behavior. Based on the analysis of their data, they argue that perhaps its origin could be found in the negative fluctuation corrections to the conductivity that we find in our calculation. It does seem plausible that the conductivity behavior near the superconducting transition tuned by varying the thickness at a fixed value of parallel magnetic field might be closely related to that tuned by varying the parallel magnetic field at a fixed value of film thickness. However, a definitive calculation catering to the former case still remains to be done. As is evident from the expression in Eq. (11), the pair-breaking parameter depends not only on the magnetic field but also on the thickness of the film. If the only effect of changing the thickness were to tune the pair-breaking strength, then the two cases would, in fact, be identical. The complication arises because tuning the thickness results also in tuning the disorder strength. Tuning the magnetic field offers a way of isolating the pair-breaking effect. More recently, Aubin *et al.*[36] have done measurements of field-tuned SIT on NbSi thin films and interpreted the data to conclude that in their experiment, the case of perpendicular field is different from that of parallel, based on the presence or absence of a kink in the temperature profile of the critical field, respectively.

It is desirable to have a systematic experimental study aimed specifically at exploring the physics of a pair-breaking quantum phase transition in superconducting films. There have been few works using a parallel field, but they have had a limited goal focusing on the SIT, as mentioned in the preceding paragraph. Amorphous (nongranular) superconducting films that are thinner than ξ, but not too thin—and are weakly disordered, with as low a sheet resistance as possible—would be necessary to assure that the quantum corrections are small enough. To begin with, it will be useful to observe the finite-temperature classical transition and verify the predictions of the fluctuation conductivity in its vicinity. By slowly increasing the pair-breaking strength and lowering the temperature, one could approach the quantum phase transition. Having identified the right films, measurements of the temperature and pair-breaking parameter (tuned by a parallel field, for example) dependence of the conductivity would afford an exciting possibility of discovering different regimes in the vicinity of the pair-breaking quantum phase transition. The increase in normal state resistance due to the presence of superconducting fluctuations that we find is in stark contrast to the intuitive expectation and is a purely quantum effect. A clear experimental signature of such a characteristically quantum behavior in the *quantum* regime, changing over into an increase in conductivity in the *classical* regime, would be an important step forward in the study of quantum phase transitions and low-temperature superconductivity. The manifestation to be expected in the plots for conductivity as a function of temperature and pair-breaking strength can be found in the previous section. The next revealing experiment would be to measure the evolution of the conductivity behavior with the change of angle made by the magnetic field with the film, ranging from parallel to perpendicular case.

Though most experiments on thin films have focused on perpendicular magnetic field and disorder-tuned transitions, recently Parker *et al.*[37] have performed measurements on homogeneously disordered ultrathin *a*-Pb films to study the magnetic-impurity-tuned transition in addition. They have compared the conductivity behavior near quantum phase transitions tuned by all three mechanisms. They have concluded that the disorder-tuned and the magnetic-impurity-tuned cases show similar behavior, which seems to be consistent with a fermionic nature of the transition to a weakly insulating normal state. Their experiment is of relevance to us since they have successfully traced the transition line and shown that it satisfies the Abrikosov-Gorkov suppression of T_c given by Eq. (1). However, the dependence of the conductivity on the magnetic impurity concentration has not been presented and the temperature dependence has been shown only for one concentration value that is above the critical concentration corresponding to α_{c0}. It will be very interesting to carry out a detailed comparison of this experiment with our theory.

Systematic experiments exploring the pair-breaking quantum phase transition tuned by magnetic impurities in three-dimensional superconductors would provide a good check of our theory, given that in this case we are above the upper critical dimension. For example, verifying the lack of quantum critical divergence as the critical impurity concentration is approached by lowering the temperature and finding the temperature-independent behavior instead would provide a contrast to the critical divergence expected in the case of one- and two-dimensional superconductors. Finding a weak nonmonotonic behavior and the presence of a quantum regime would be interesting in its own right. In addition, the analysis of the transition in a relatively simple material would provide useful insights in interpreting the behavior

near the superconducting quantum phase transitions in more complex materials.

As far as superconducting quantum phase transition and quantum corrections are concerned, a lot of theoretical as well as experimental work on disordered thin films has been carried out over the period of the last two decades. Relatively less work on similar lines has been done on superconducting wires. However, the technological advance allowing for the fabrication of superconducting nanowires that are uniform and ultrathin (<10 nm) (see, e.g., Ref. 38) has invigorated the field and opened up different possibilities. By coating carbon nanotubes or DNA molecules suspended over a trench with a superconducting alloy such as MoGe or Nb, one essentially obtains superconducting wires connected on two sides to thin-film electrodes of the same material. So far, most experiments done on this setup have focused on unraveling the physics of phase-slip fluctuations that result in a nonzero resistance below the superconducting transition. In one recent experiment, Rogachev *et al.*[39] have looked at the effect of magnetic fields. They were able to explain the suppression of the transition temperature in terms of the pair-breaking theory [Eq. (20)] if the Zeeman pair-breaking effect in the presence of spin-orbit coupling was taken into account in addition to the orbital effect of the magnetic field applied perpendicular to the wire [see Eq. (15)]. Although the fluctuation effects above the transition were not explored until now, we believe that the experimental setup is appropriately geared to be able to test the predictions of our theory. Systematic study of low-temperature fluctuations both below and above the transition would be essential not only to understand the nature of mesoscopic superconductivity but also to be able to successfully control superconducting electronic circuits involving ultranarrow wires.

The parallel-magnetic-field-tuned quantum phase transition in doubly connected superconducting cylinders that we discuss in Sec. II—with the pair-breaking parameter given by Eq. (19)—has been motivated by its experimental realization by Liu *et al.*[40] They clearly seem to have observed the enhancement of the conductivity resulting from the positive fluctuation contribution in the classical regime. However, so far there has been no experimental evidence of the corrections expected in the intermediate and quantum regimes. Further experiments in this direction would be very interesting.

In conclusion, we have evaluated the fluctuation corrections to the electrical conductivity in the vicinity of the pair-breaking quantum phase transition using diagrammatic perturbation theory in disordered systems by correctly incorporating the quantum fluctuations within the formalism. Among the three distinct superconducting fluctuation regimes that we find, the quantum regime is the one in which the contributions to the conductivity coming from the interaction between the fluctuating pairs and normal electrons are important, while the behavior in the classical (or quantum critical) and the intermediate regime is dominated by direct transport via the fluctuating pairs. Our theory thus seems to indicate that the effective bosonic action formalism should be applicable outside the quantum regime.[41] It should be noted that even at zero temperature, our theory is expected to be valid only outside the quantum Ginzburg region for systems below or at the upper critical dimension. One important open problem is to understand in what way the zero-temperature conductivity above the transition connects with that below the transition.

Within our microscopic theory, we have been able to extract the finite-temperature crossovers to be expected near the superconducting quantum critical point. We have used the electrical conductivity as a means of probing the effects of superconducting fluctuations; however, a similar analysis could also be carried out for the diamagnetism and other thermodynamic quantities. Extension to the case of anisotropic superconductors such as high-temperature superconductors would also be interesting. In *d*-wave superconductors, disorder acts as a pair breaker and the behavior near the corresponding pair-breaking quantum phase transition is likely to have some resemblance to our findings.

We believe that pair-breaking quantum phase transitions form an important class of quantum phase transitions that not only allow for a systematic, well-controlled experimental exploration but also provide the possibility of a thorough and comprehensive theoretical analysis. We hope that our work has amply demonstrated the latter and will, in turn, motivate the former. In the end, we expect that the microscopic theory of the superconducting quantum critical point and the corresponding experimental analysis would serve as a useful prototype for understanding quantum phase transitions also in other classes of correlated systems.

ACKNOWLEDGMENTS

One of the authors (N.S.) would like to gratefully acknowledge Alexey Bezryadin, Allen Goldman, and Kevin Parendo for discussions regarding experiments and NSF Grant No. DMR 0605813 for financial support while part of the work was carried out.

[1] S. L. Sondhi, S. M. Girvin, J. P. Carini, and D. Shahar, Rev. Mod. Phys. **69**, 315 (1997).
[2] S. Sachdev, *Quantum Phase Transitions* (Cambridge University Press, Cambridge, England, 2001).
[3] M. Tinkham, *Introduction to Superconductivity* (McGraw-Hill, New York, 1996).
[4] P. G. de Gennes, *Superconductivity of Metals and Alloys* (Benjamin, New York, 1966).
[5] W. J. Skocpol and M. Tinkham, Rep. Prog. Phys. **38**, 1049 (1975).
[6] A. I. Larkin and A. A. Varlamov, *The Physics of Superconductors* (Springer-Verlag, Berlin, 2003).
[7] P. W. Anderson, J. Phys. Chem. Solids **11**, 26 (1959).
[8] A. A. Abrikosov and L. P. Gor'kov, Sov. Phys. JETP **12**, 1243 (1961).
[9] K. D. Usadel, Phys. Rev. Lett. **25**, 507 (1970).

[10] N. Kopnin, *The Theory of Nonequilibrium Superconductivity* (Oxford University Press, Oxford, 2001).
[11] A. A. Abrikosov, L. P. Gorkov, and I. E. Dzyaloshinski, *Methods of Quantum Field Theory in Statistical Physics* (Dover, New York, 1975).
[12] B. L. Altshuler and A. G. Aronov, *Electron-Electron Interactions in Disordered Conductors*, edited by A. L. Efros and M. Pollak (Elsevier Science, Amsterdam, 1985), Chap. 1, pp. 1–153.
[13] L. P. Gorkov, A. I. Larkin, and D. E. Khmelnitskii, JETP Lett. **30**, 228 (1979).
[14] B. L. Altshuler, A. G. Aronov, and P. A. Lee, Phys. Rev. Lett. **44**, 1288 (1980).
[15] K. Efetov, *Supersymmetry in Disorder and Chaos* (Cambridge University Press, Cambridge, England, 1997).
[16] L. G. Aslamazov and A. I. Larkin, Sov. Phys. Solid State **10**, 875 (1968).
[17] K. Maki, Prog. Theor. Phys. **40**, 193 (1968).
[18] R. S. Thompson, Phys. Rev. B **1**, 327 (1970).
[19] R. S. Thompson, Physica (Amsterdam) **55**, 296 (1971).
[20] R. Ramazashvili and P. Coleman, Phys. Rev. Lett. **79**, 3752 (1997).
[21] A. J. Millis, Phys. Rev. B **48**, 7183 (1993).
[22] V. P. Mineev and M. Sigrist, Phys. Rev. B **63**, 172504 (2001).
[23] I. F. Herbut, Phys. Rev. Lett. **85**, 1532 (2000).
[24] J. A. Hertz, Phys. Rev. B **14**, 1165 (1976).
[25] I. S. Beloborodov and K. B. Efetov, Phys. Rev. Lett. **82**, 3332 (1999).
[26] I. S. Beloborodov, K. B. Efetov, and A. I. Larkin, Phys. Rev. B **61**, 9145 (2000).
[27] V. M. Galitski and A. I. Larkin, Phys. Rev. B **63**, 174506 (2001).
[28] A. V. Lopatin, N. Shah, and V. M. Vinokur, Phys. Rev. Lett. **94**, 037003 (2005).
[29] D. B. Haviland, Y. Liu, and A. M. Goldman, Phys. Rev. Lett. **62**, 2180 (1989).
[30] M. P. A. Fisher, Phys. Rev. Lett. **65**, 923 (1990).
[31] V. F. Gantmakher, S. N. Ermolov, G. E. Tsydynzhapov, A. A. Zhukov, and T. I. Baturina, JETP Lett. **77**, 424 (2003).
[32] T. I. Baturina, D. R. Islamov, J. Bentner, C. Strunk, M. R. Baklanov, and A. Satta, JETP Lett. **79**, 337 (2004).
[33] P. W. Adams, Phys. Rev. Lett. **92**, 067003 (2004).
[34] V. F. Gantmakher, M. V. Golubkov, V. T. Dolgopolov, A. Shashkin, and G. E. Tsydynzhapov, JETP Lett. **71**, 473 (2000).
[35] K. A. Parendo, L. M. Hernandez, A. Bhattacharya, and A. M. Goldman, Phys. Rev. B **70**, 212510 (2004).
[36] H. Aubin, C. A. Marrache-Kikuchi, A. Pourret, K. Behnia, L. Berge, L. Dumoulin, and J. Lesueur, Phys. Rev. B **73**, 094521 (2006).
[37] J. S. Parker, D. E. Read, A. Kumar, and P. Xiong, Europhys. Lett. **75**, 950 (2006).
[38] A. Bezryadin, C. N. Lau, and M. Tinkham, Nature (London) **404**, 971 (2000).
[39] A. Rogachev, A. T. Bollinger, and A. Bezryadin, Phys. Rev. Lett. **94**, 017004 (2005).
[40] Y. Liu, Y. Zadorozhny, M. M. Rosario, B. Y. Rock, P. T. Carrigan, and H. Wang, Science **294**, 2332 (2001).
[41] A. Del Maestro, B. Rosenow, N. Shah, and S. Sachdev, arXiv:0708.0687v1.